

NYO-9072
AEC Research and
Development Report
UC-81, Power Reactors

COOLBALL

**A Machine Code for Thermal
Analysis of Pebble Bed Reactor
Cores**

Work Performed Under AEC Contract AT(30-1)-2207

**SANDERSON & PORTER
New York, N. Y.**

TABLE OF CONTENTS

	<u>Page</u>
1.0 Introduction	1
2.0 Pebble Bed Fluid Dynamics	3
3.0 Machine Program	9
4.0 Illustrative Problem	14

List of Figures

<u>Figure No.</u>	<u>Title</u>	<u>Following Page</u>
2.1	Typical PBR Fuel Elements.....	3
2.2	Formal Packing Arrangements of Spheres.....	3
2.3	Void Fraction Distribution in Beds & in an Annulus.....	4
2.4	Integrated Void Distribution in Packed Beds.....	5
2.5	Voidage vs. d/D_p	5
2.6	Friction Factor Correlation for Packed Beds.....	6
2.7	Heat Transfer Correlation for Packed Beds.....	7
3.1	Calculation Flowsheet COOLBALL I.....	10
3.2	Operating Instructions COOLBALL I.....	10
3.3	Calculation Flowsheet COOLBALL II.....	13
3.4	Operating Instructions COOLBALL II.....	13
4.1	Axial & Radial Power Distribution in PBR Core.....	14
4.2	Gas Flow Distribution in PBR Core.....	15
4.3	Bulk Gas Temperature vs. Axial Position in Core.....	15
4.4	Outlet Gas Temperature Distribution in Radial Direction	15
4.5	Gas & Average Solid Temperatures in Core.....	15
4.6	Percent of Core at or above Any Temperature.....	15
4.7	Graphite Surface & Center Temperatures in Core.....	15

List of Tables

<u>Table No.</u>	<u>Subject</u>	<u>Following Page</u>
3.1	Input & Output Card Format COOLBALL I	10
3.2	Program Listing (Five-per-Card) COOLBALL I.....	10
3.3	Input & Output Card Format COOLBALL II	13
3.4	Program Listing (Seven-per-Card) COOLBALL II.....	13
4.1	Characteristics of 750 tMW Pebble Bed Reactor	see 14
4.2	COOLBALL I Complete Input & Output for 750 tMW PBR Core	14
4.3	COOLBALL II Complete Input & Output for 750 tMW PBR Core	14

COOLBALL

A Machine Code for Thermal Analysis of Pebble Bed Reactor Cores.

Abstract

COOLBALL is an IBM 650 machine program designed to calculate local gas and ball temperatures, gas flow, and pressure loss as induced by non-uniform power generation and voidage within an axial flow Pebble Bed Reactor core. This code has been used extensively to study the thermal characteristics of Pebble Bed Reactor cores in support of a broad program for the development of the PBR concept.

Section 1.0 Introduction

This report presents the details in the development and application of a machine program named COOLBALL, which has been instrumental in demonstrating that there are no flow instabilities in a Pebble Bed Nuclear Reactor core. This work was prompted by reports that flow instabilities had been observed in a number of packed bed chemical reactors which possessed operating characteristics similar in certain respects to those of a nuclear reactor. Some support for the persistent rumors of flow instability can be found in the fundamental correlation for pressure drop in compressible fluids. These relationships indicate that the specific pressure drop will be higher in regions of high temperature than in regions of low temperature. This would cause flow divergence from the high temperature zone which would cause the temperature to rise to higher levels which would accentuate the flow divergence and so on.

Analysis of this problem is complicated by the fact that specific flow paths through a packed bed defy description and, whereas locally conditions may differ from the average, one must average these differences before calculations can be made. Adding to the complications is the cyclicly varying voidage which has been found to exist in packed beds of uniformly sized particles in regions adjacent to container walls. These complications and the feedback effect referred to above indicated that a numerical-iterative approach would be required.

This approach of dividing the core into a number of regions, each of which was assumed to be homogeneous, with step changes between adjacent

regions was tried and found to be satisfactory. To achieve significance in the results, relatively many subdivisions are required.

Unfortunately the practical limitations of hand calculations ruled out anything but coarse grid structures with few subdivisions. Obviously by programming the calculations for machine solution much finer meshes could be studied and results could be obtained in reasonable times, thereby eliminating the dilemma entirely.

In addition to the analysis of the fluid dynamics of pebble beds and the details of the machine program, this report contains a fully developed example problem in Section 4.0.

Section 2.0 Pebble Bed Fluid Dynamics

The Pebble Bed Reactor core consists of a randomly packed, static bed, of spherical uranium-graphite fuel elements of a type as illustrated in Figure 2.1. These elements contain fissile and/or fertile material as a ceramic and provide the moderator and heat transfer surface in the reactor.

2.1 Packing of Spheres

The packing of spheres in a pebble bed is of prime interest in the use of this configuration as a reactor core. In 1935, Graton & Fraser (1) made a thorough study of the stacking of spheres and concluded that there are four formal stacking arrangements having voidages which vary from 26% in the case of the rhombohedral packing to 48% in the case of cubic packing as shown in Figure 2.2, and its associated table. It should be noted that there are two orthorhombic and two rhombohedral cases listed in the table. These cases are identical as far as the arrangement of spheres is concerned but differ in their orientation with respect to the major axis of flow. Martin et al (2) have shown that this anisotropy is unimportant in the case of the rhombohedral packing but is important in the case of the orthorhombic packing.

Another method of recognizing the regular packing configuration is by the arrangement and number of tangent neighbors associated with each sphere. Twelve points of contact are typical of rhombohedral packing while cubic packing has only six.

Actually a packed bed prepared in a random fashion could not be as ordered as implied in Figure 2.2. Smith et al (3) based on a study of ball contact points concluded that a randomly packed bed could be considered as a mixture of simple cubic and rhombohedral packing configurations. More recently Wadsworth (4) in a carefully executed study of contact

(1) Graton, L.C. & Fraser, H.J. *J. Geol.* 43 785 & 910 (1935)

(2) Martin, J.J., McCabe, W.L. & Monrad, C.C., *Chem. Eng. Prog.* 47 91 (1951)

(3) Smith, W.O., Foote, P.D., Busang, P.F., *Phys. Rev.* 34 1271 (1929)

(4) Wadsworth, J. *Nat. Res. Council of Canada, Report MT-41* (1960)



TYPICAL FUEL ELEMENTS FOR THE PEBBLE BED REACTOR

FIG. 2.1



CUBIC

ORTHORHOMBIC

TETRAGONAL

RHOMBOHEDRAL

FORMAL PACKING ARRANGEMENTS OF SPHERES

Layer Type	Square			Rhombic		
	I	II	III	IV	V	VI
<u>Geometrical Relationship</u>						
Name	Cubic	Orthorhombic	Rhombohedral	Orthorhombic	Tetragonal	Rhombohedral
Spacing of Layers	$R\sqrt{4}$	$R\sqrt{3}$	$R\sqrt{2}$	$R\sqrt{4}$	$R\sqrt{3}$	$2R\sqrt{2/3}$
Tangent Neighbors	6	8	12	8	10	12
<u>Properties</u>						
Volume of Unit Cell	$8.00R^3$	$6.93R^3$	$5.66R^3$	$6.93R^3$	$6.00R^3$	$5.66R^3$
Volume of Unit Void	$3.81R^3$	$2.74R^3$	$1.47R^3$	$2.74R^3$	$1.81R^3$	$1.47R^3$
Voidage - %	47.64	39.54	25.95	39.54	30.19	25.95

FIG. 2.2

points, using a technique similar to that of Smith, has shown that all randomly produced packing configurations tend toward rhombohedral. Thus a sphere having fewer than 12 contact points is experiencing rhombohedral packing with one, two or more contacts missing, i. e. an incomplete rhombohedral array. Wadsworth concludes that in a randomly packed bed of hard, smooth homogeneous spheres, the local packing configuration is incomplete rhombohedral with the degree of incompleteness randomly distributed throughout the bed.

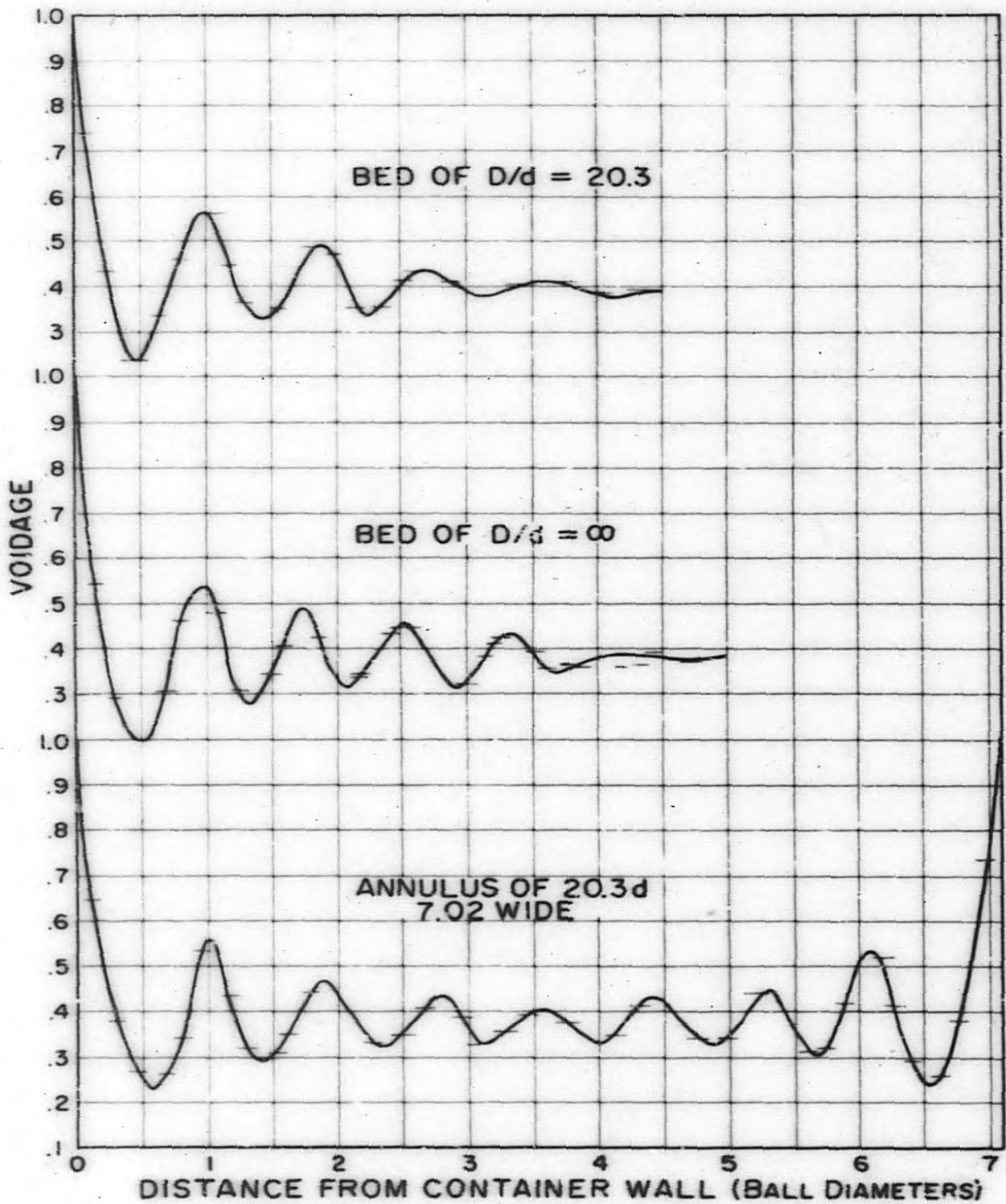
2.2 Void Distribution

The most highly oriented region of a ball bed exists adjacent to container walls and any other smooth surfaces which may exist within the bed. These surfaces result in a radial variation of voidage within a bed of randomly packed spheres which varies from 100% at the surface to about 37% at a distance determined to be about five ball diameters in from the surface. This variation was determined (5) by an experimental technique which consisted of pouring lead shot into a cylindrical mold and filling the void with epoxy resin which upon curing resulted in a packed bed, fixed within a cylinder. This cylinder was then machined to successively smaller diameters and the density of each annular ring which was machined off was determined. Knowledge of the densities of the plastic and lead permit one to determine the relative volume of plastic and lead and hence the voidage in each annular ring.

Three sets of detailed results for a bed having a d/D_p ratio of ∞ , 20.3 and an annular ring of $7.025 D_p$ in width, are shown in Figure 2.3.

These data show the maximum voidage at the interface between the outermost row of spheres and the wall. Proceeding in from the wall, the voidage decreases to a minimum at half a ball diameter, after which it starts to increase. It cannot increase to unity, however, since the second row of spheres rests in cusps between the spheres in the first row. Proceeding in from the first row the pattern is repeated and since each row is more random than the row which precedes it, the voidage oscillates with a decreasing amplitude around a mean value. These oscillations are not completely damped out until a point is reached about five ball diameters in from the wall.

(5) Benenati, R. F. & Brosilov, C. A. I. Ch. E. Journal, 7 (1961)



VOID FRACTION DISTRIBUTION IN BEDS & AN ANNULUS

FIG. 2.3

The presence of a convex wall in a bed, such as would result from a graphite column containing control rods, has the same effect as concave surfaces on the orientation of balls adjacent to it. This is shown in the lowest curve of Figure 2.3 which shows the void distribution in an annulus about 7 ball diameters wide. It should be noted that unless such solid surfaces within a bed are spaced quite far apart, say 15 ball diameters, the average voidage in such a bed will be greater than the voidage in a bed not so perturbed.

Figure 2.4 shows the integrated voidage as a function of the ratio of bed diameter to ball diameter and the distance from the wall, based on the above-mentioned void distribution studies. It can be seen that for small beds or beds of large particles ($d/D_p < 20$) the average void fraction is generally higher than the often-quoted 39%. This is also shown in Figure 2.5 (6), which shows that the voidage in a packed bed of uniform spheres is independent of the sphere diameter but is a function of the ratio of bed to sphere diameter. Wadsworth (4) who has experimentally confirmed this plot of Carman's has concluded that the wall voidage accounts for nearly all the voidage change with increasing container size since the packing configuration (incomplete rhombohedral) is not effected by container size.

2.3 Fluid Friction Characteristics

Dimensional analysis of the problem of determining the total pressure drop through randomly packed beds of spherical particles where the bed has an appreciable depth leads to the expression:

$$\frac{\Delta p g D_p}{\rho L v_s^2} = F \left[\frac{D_p v_s \rho}{\mu}, \epsilon, \frac{e}{D_p}, \frac{d}{D_p}, \beta \right] \quad (1)$$

where:

Δp is the total pressure drop through the bed
 v_s the superficial fluid velocity, referred to the total face area of the bed

D_p is the particle diameter

L is the bed length

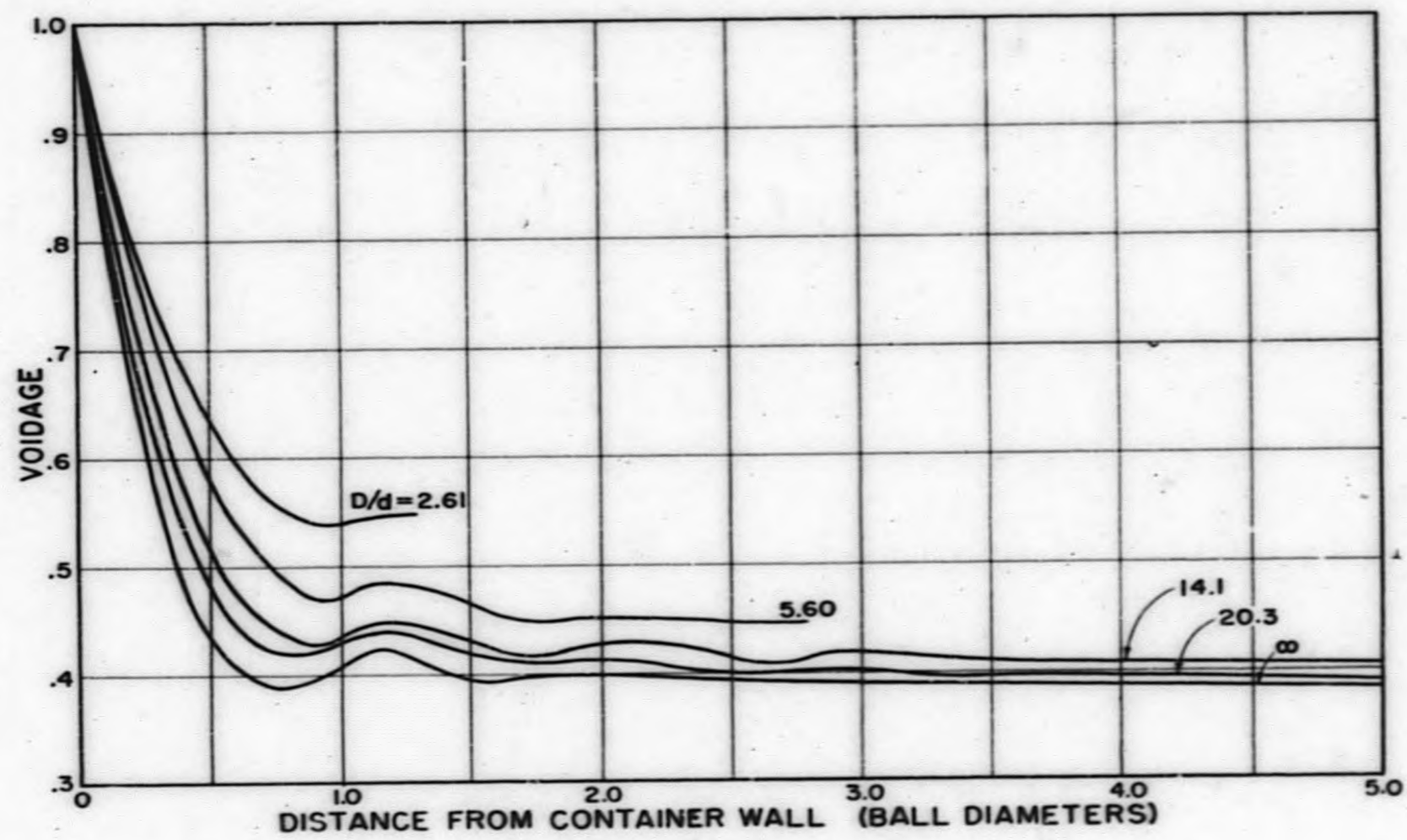
ϵ is the voidage

e is a representative dimension of surface finish

d is the bed or container diameter

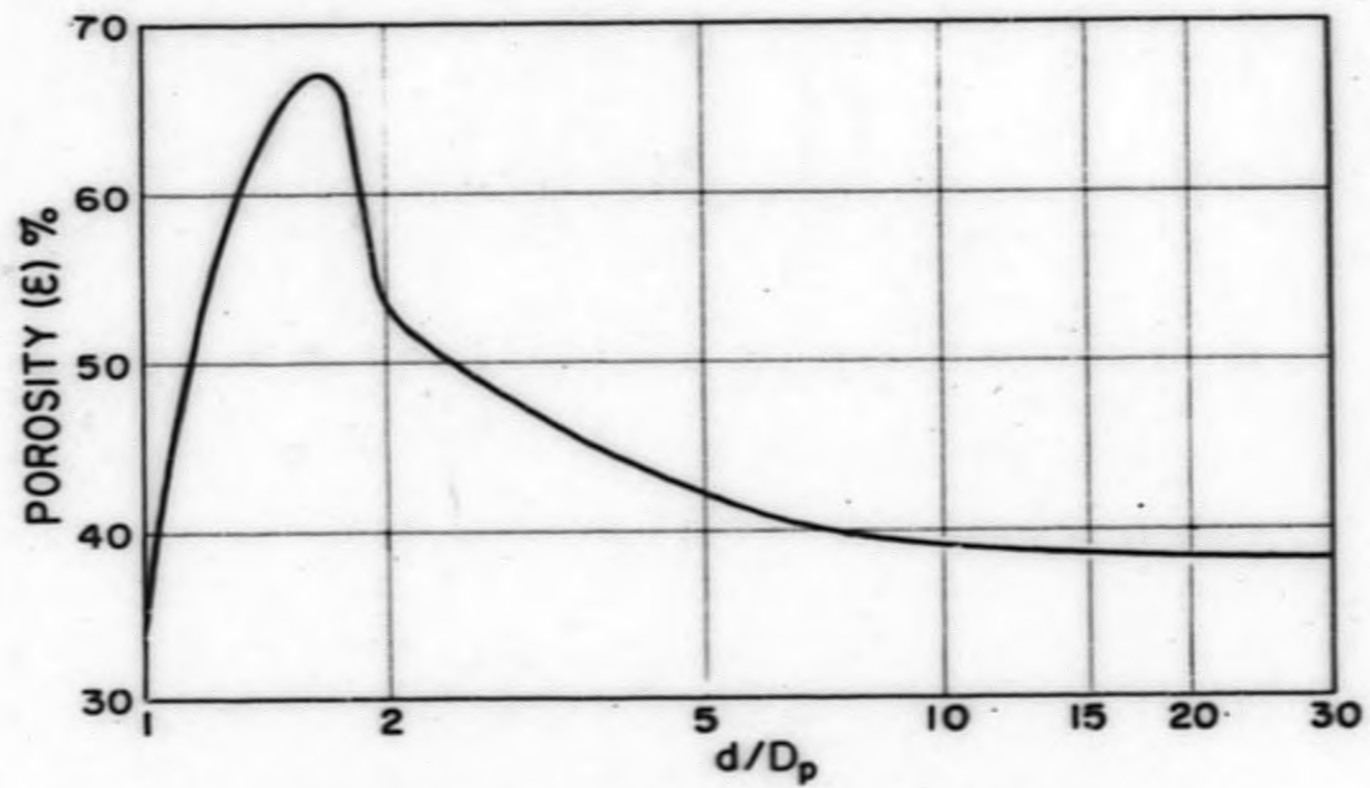
β is the loss associated with entrance and exit effects

(6) Carman, P. C. Trans. A. I. Ch. E. 15 (1937)



INTEGRATED VOID FRACTIONS

FIG. 2.4



CARMAN'S RELATION BETWEEN POROSITY OF
BED & SIZE OF CONTAINER

FIG. 2.5

Pressure drop through beds of randomly packed spheres is usually correlated by plotting a modified friction factor f' vs. a modified Reynolds number Re' , defined as follows:

$$f' = \frac{\Delta P}{L} \frac{\rho g D_p}{2 G_s^2} \frac{\epsilon^3}{(1-\epsilon)} \quad (2)$$

$$Re' = \frac{D_p G_s}{\mu(1-\epsilon)} \quad (3)$$

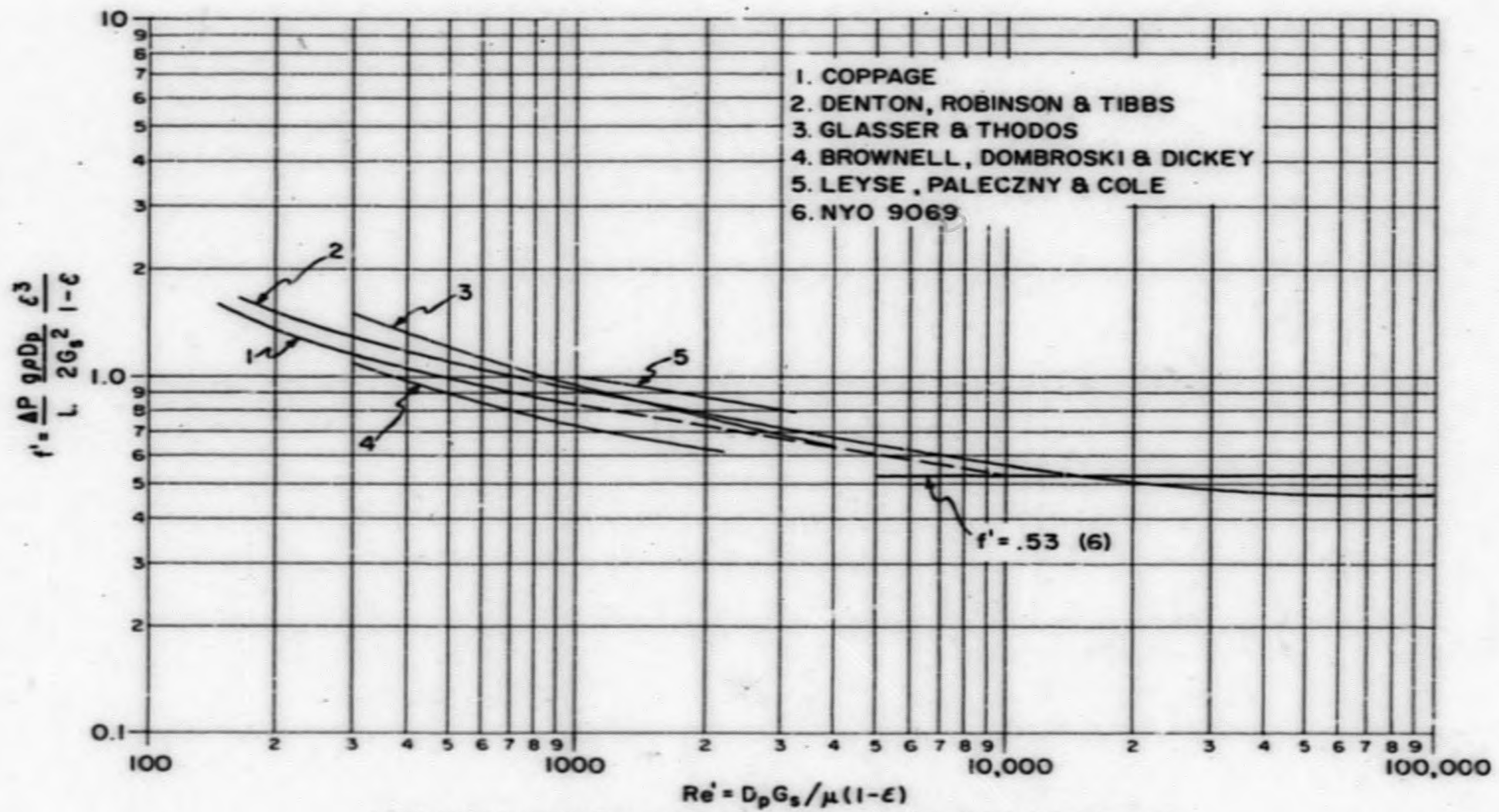
where G_s is the superficial mass flow through the bed, i.e. $G_s = v_s \rho$.

Figure 2.6 presents a plot of friction factor f' vs Reynolds number Re' for beds of randomly packed spheres as determined by a number of investigators. In general these data were obtained in beds where D_p was quite small and the ratio of d/D_p quite large. The data of curve #6 were obtained (7) using 3/4" and 1-1/2" diameter balls in beds approximately 7-1/2" and 15" diameter for a d/D_p of 10 and 20. The data of curve #2 were also obtained (8) using relatively large spheres.

These two sets of results are in excellent agreement in that both show friction factor to be independent of Reynolds number in the high range. The principal difference is that the work reported on in NYO-9069 shows the friction factor to be independent of Reynolds number, to values about one order of magnitude lower than shown in (8)

It has been recommended (9) that a value of f' of 0.53 be used for design of Pebble Bed Reactor cores where the bed has a $d/D_p \geq 20$ and modified Reynolds number is ≥ 5000 . This value of f' has therefore been used in developing the program described in this report.

- (7) NYO-9069 Pebble Bed Friction Factor & Thermal Expansion Tests
- (8) HPC-35 Heat Transfer & Pressure Loss in Fluid Flow through Randomly Packed Spheres
- (9) NYO-9071 Progress Report-Pebble Bed Reactor Program



FRICITION FACTOR CORRELATION FOR PEBBLE BEDS

FIG. 2.6

2.4 Heat Transfer Characteristics

Figure 2.7 presents a heat transfer correlation for pebble bed from the data obtained by three investigators. These data are presented in terms of a heat transfer grouping j_s , defined as:

$$j_s = h Pr^{.66} / G_s C_p \quad (4)$$

and a modified Reynolds number Re' defined as:

$$Re' = D_p G_s / \mu (1 - \epsilon) \quad (5)$$

The data of principal interest is that of Coppage (10) and Denton (8). The results of Coppage were found to be represented by the following expression:

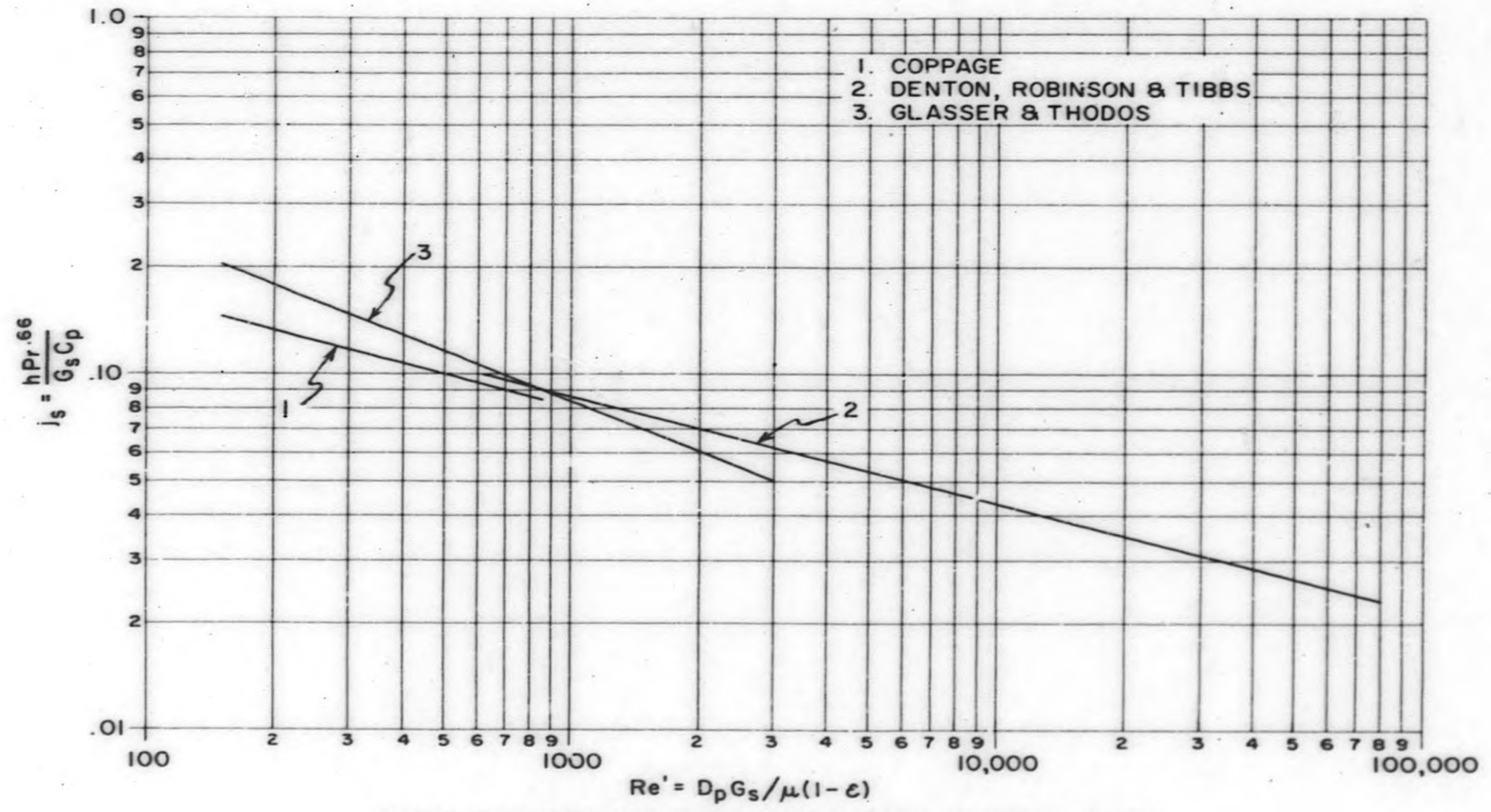
$$\frac{h Pr}{G_s C_p} = \frac{0.21}{\left(\frac{D_p G_s}{\mu}\right)^{.31}} \quad \text{for } 25 < Re < 550 \quad (6)$$

for a bed of voidage of 39%.

It will be noted that the data are reduced in terms of the mass flow through the interstices of the bed itself and the hydraulic diameter of the flow passage. The data can also be expressed in terms of mass flow at the face of the bed (G_s), particle diameter (D_p), and modified Reynolds number (Re'), and made applicable for any gas, as follows:

$$j_s = \frac{h Pr^{.66}}{G_s C_p} = \frac{0.68}{\left[\frac{D_p G_s}{\mu(1-\epsilon)}\right]^{.31}} \quad (7)$$

(10) TR-No. -16 Heat Transfer & Flow Friction Characteristics
of Porous Media - Stanford University



HEAT TRANSFER CORRELATION FOR PEBBLE BEDS

FIG. 2.7

The results of Denton were found to be represented by the following expression:

$$\frac{h}{G_s C_p} = \frac{0.72}{\left(\frac{D_p G_s}{\mu}\right)^{.3}} \quad (8)$$

at a value of Pr of 0.73 and voidage of 37%. Expressing in terms of $\frac{h Pr^{.66}}{G_s C_p}$ and in terms of the modified Reynolds number Re' :

$$j_s = \frac{h Pr^{.66}}{G_s C_p} = \frac{0.677}{\left[\frac{D_p G_s}{\mu(1-\epsilon)}\right]^{.3}} \quad (9)$$

The correlation of these data is remarkable, considering that the tests were run by different laboratories at different times and over different Reynolds number ranges. One piece of data is simply an extension of the other and in view of the fact that the bulk of the data is that of Denton, we choose to represent the mean by the expression:

$$j_s = \frac{0.68}{Re'^{.03}} \quad 100 < Re' < 80,000 \quad (10)$$

The data of Glasser & Thodos (11) is included in Figure 2.7 because their results were obtained simultaneously with their friction factor results in Figure 2.6. Their values of j_g at the extreme of the range tested bracket the Coppage-Denton data.

To allow for spread in experimental data and to insure that maximum specified temperatures will not be exceeded, it has been recommended (9) that j_g be reduced by 15% for design purposes, or

$$j_g = .58/Re'^{0.3}$$

which is the value that has been used in developing the program described in this report.

- (11) Glasser & Thodos Heat & Momentum Transfer in the Flow of Gases through Packed Beds - Ph.D. Thesis Northwestern Technical Institute

Section 3.0 Machine Program

A characteristic of a Pebble Bed Reactor core is that its coolant flow passages are interconnected radially as well as axially. This gives rise to radial coolant flow components which are effected by radial variation in temperature and voidage. Radial temperature variations stem from the radial power distribution while radial voidage distributions stem from the effect of the bed boundaries. Roughly parallel situations arise in chemical reactors in which catalized exothermic reactions take place in packed beds.

3.1 Problem Analysis

The technique employed for thermal and flow analysis consists of dividing the bed into annular rings and axial slices with the assumption that the system is homogeneous within each matrix cell resulting from this subdivision. Radial flow between adjacent matrix cells is only permitted at the boundaries of axial slices and it is assumed that there is no resistance to radial flow at these points, i.e. the pressure is constant across any axial slice. The flow in each matrix cell is determined in an interative process for each layer. The analysis proceeds layer by layer in the gas flow direction.

The problem was further subdivided into one program which developed the local heat generation rates and a second program which analyzes the flow and temperatures resulting therefrom.

3.2 Code Details

COOLBALL (parts I and II) is an IBM 650 machine code designed to solve for local gas and ball temperatures, gas flow and pressure loss as induced by non-uniform power generation and voidage within an axial flow Pebble Bed Reactor core. Input data required for COOLBALL I are normalized radial and axial power distribution and gross power. COOLBALL II requires the system pressure, flow rate, fuel element size, matrix cell dimensions, certain thermodynamic properties of the gas as detailed later, and the complete output of COOLBALL I.

3.2.1 COOLBALL I

Before using the code, unit cells are established by dividing the core into a convenient number of annular rings (not to exceed 20) and axial layers (not to exceed 20). Voidage distribution is established, based on d/D_p ratio of the bed or any perturbations in voidage that are to be introduced. Weight flow through the core is determined from the specified power output and temperature rise through the core. COOLBALL I generates an average power output for each matrix cell from the radial and axial power distribution. The input power distribution may be in the form of ratios of local to average power or ratios of local to peak power. The core specific power (BTU/sec/ft³ bulk bed) may be the average or peak value but must be compatible with the power distribution.

The program was written for the basic 650 using FORTRANSIT I. All data must therefore be floating point numbers in the form .XXXXXXXXYY where XXXXXXXX represents the eight most significant figures and YY is 50 plus the power of ten needed to relocate the decimal point.

Table 3.1 lists the card format for input and output to COOLBALL I.

Figure 3.1 shows the calculation flow sheet for this program.

Table 3.2 lists the last 15 cards of the program deck in the standard 5 word per card format. This deck must, of course, be preceded by the 85 card SOAP-PACKAGE deck which contains the FORTRANSIT interpretive routines which are common to all FORTRANSIT programs.

Figure 3.2 indicates the operating instructions for COOLBALL I.

3.2.2 COOLBALL II

In COOLBALL II, analysis proceeds layer by layer in the gas flow direction. As a start, the local mass velocity for each matrix cell of the first layer is assumed to equal the average mass velocity which is read in as input. The local temperature rise in each matrix cell of the first layer is determined from a heat balance over the cell, and the arithmetic mean temperature in the cell is computed. Gas Properties in the cell

TABLE 3.1

CARD FORMAT COOLBALL PART I

INPUT

Card								CC73
1	RP ₁	RP ₂	RP ₃	RP ₄	RP ₅	RP ₆	RP ₇	+
2	RP ₈	RP ₉	RP ₁₀	RP ₁₁	RP ₁₂	RP ₁₃	RP ₁₄	+
3	RP ₁₅	RP ₁₆	RP ₁₇	RP ₁₈	RP ₁₉	RP ₂₀	\bar{Q} or Q _{max} *	+
4	AP ₁	blank	blank	blank	blank	blank	blank	+
5	AP ₂	blank	blank	blank	blank	blank	blank	+
23**	AP ₂₀	blank	blank	blank	blank	blank	blank	+

OUTPUT

1	Q _{1,1}	Q _{2,1}	Q _{3,1}	Q _{4,1}	Q _{5,1}	Q _{6,1}	Q _{7,1}	blank
2	Q _{8,1}	Q _{9,1}	Q _{10,1}	Q _{11,1}	Q _{12,1}	Q _{13,1}	Q _{14,1}	blank
3	Q _{15,1}	Q _{16,1}	Q _{17,1}	Q _{18,1}	Q _{19,1}	Q _{20,1}	blank	blank
4	Q _{1,2}	Q _{2,2}	Q _{3,2}	Q _{4,2}	Q _{5,2}	Q _{6,2}	Q _{7,2}	blank
60	Q _{15,20}	Q _{16,20}	Q _{17,20}	Q _{18,20}	Q _{19,20}	Q _{20,20}	blank	blank

* If power profiles are normalized to max. power = 1.0, Q_{max} must be used; if however power profiles are normalized to avg. power = 1.0, \bar{Q} must be used.

** If fewer than 20 axial layers are used, unnecessary axial power input cards may be eliminated and correspondingly fewer output cards will be produced.

TABLE 3.2
COOLBALL I LISTING IN FIVE-PER-CARD FORM

78422110085	201	6500520057	2019680071	6500740079	2019690072	199900	5700710079
78422110087	6500750129	6900821913	203	6500850089	2019680121	72012900	820089
78422110088	650011240179	6901321913	202	6501350139	2000440047	121017900	1320139
78422110089	65002000066	69000500055	20000000053	6500440049	3500040059	59004700	5500530049
78422110090	150004200067	69000000002	24000210125	65000204	6500420097	59006700	6200000125
78422110091	25000430147	20000000054	6901001902	2019660069	6500440099	54009701	4701000069
78422110092	35000440109	1501128002	6500010105	2000000103	6519660171	99010901	1201050103
78422110093	650011741902	65000440149	3500040159	1501620117	69000008002	171017401	4901590117
78422110094	24000210155	1	65000020107	2000020155		162000001	401070000
78422110095	25013350189	1500440199	20000440197		6680020205	155018901	9900000197
78422110096	1500580063	4600660047	2	6501190073	2019680221	205006300	560073
78422110097	6502740229	6901821907	206	2320082	203	221022900	1820000
78422110098	800080000		20	10002	200021	232005000	5802740119
78422110099			42	20021	200001	135012400	8500750074
78422110100	41	10023	42	20021	1999	520000000	1980

NOTE: The above listing does not include the FORTRANSIT interpretive routines which are common to all FORTRANSIT programs.

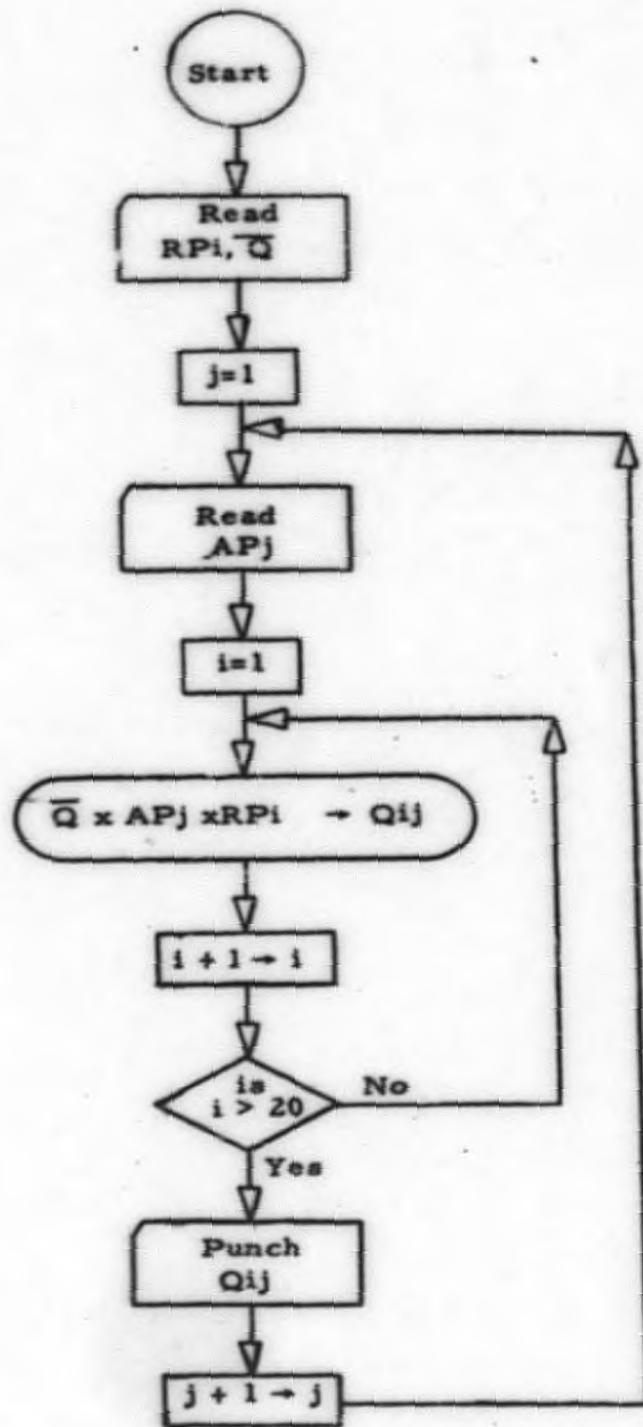
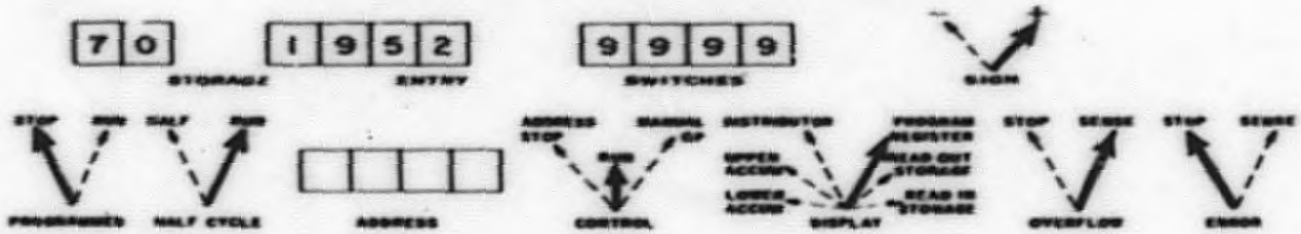


Figure 3.1
 Calculation Flow Sheet
 COOLBALL Part I

COOLBALL I

IBM 650 PROGRAM OPERATING INSTRUCTIONS



i. Initial Console Setting as shown above.

- A. Normal Starting Procedure: Computer Reset; Program Start.
- B. Special Instructions: None

ii. Card Input - Output (533 or 537)

READ FEED	
NO. OF CARDS	FILE DESCRIPTION
100	PROGRAM DECK
	DATA DECK (see below)

PUNCH FEED	
CARD FORM	
80 - 80	

CONTROL PANELS	
FORTTRANSIT II	

iii. Other Instructions and Remarks:

NOTE: Only one set of data may be loaded at a time

iv. Program Stops and Required Action:

STOP ADDRESS	MESSAGE - EXPLANATION - ACTION
	None

FIG. 3.2

are determined from the following equations:

$$\rho = \frac{PMW}{RT} \quad (11)$$

$$C_p = \bar{C}_p (T/T')^{C_{pX}} \quad (12)$$

$$\mu = \bar{\mu} (T/T')^{\mu X} \quad (13)$$

$$Pr = \bar{Pr} (T/T')^{PrX} \quad (14)$$

The appropriate exponents have to be determined in advance for the gas in question. The local mass velocity through each matrix cell is then determined from:

$$G = \left[\frac{g \rho D_p \Delta p \epsilon^3}{2 f' L (1-\epsilon)} \right]^{.5} \quad (15)$$

As was indicated earlier, a constant value of $f' = 0.53$ was used. Substituting the ideal gas law density gives:

$$G = \left[\frac{g PMW D_p \Delta p \epsilon^3}{2 RT f' L (1-\epsilon)} \right]^{.5} \quad (16)$$

which upon removal of all terms which are constant in any axial layer becomes:

$$G = \text{CONST} \left[\frac{\epsilon^3}{T(1-\epsilon)} \right]^{.5} \quad (17)$$

where T is the local average temperature in each matrix cell in the given axial layer. Using just the argument of the square root in equation (17), the relative mass velocity in each matrix cell of a given layer is determined. For each axial layer, a mass balance prescribes that:

$$W = \sum G_i A_i \quad (18)$$

from which actual mass velocities in each cell are determined. The new mass velocities are used to compute new local average temperatures and the operation repeated until a predetermined agreement is reached between the assumed and calculated mass velocities.

The corrected local gas outlet temperatures and pressure of the preceding layer furnish the inlet conditions for the next layer, the corrected mass velocities of the preceding layer serve as first assumptions for mass velocities in the next layer and so on until the entire core is traversed.

For each layer, mixed mean outlet temperature is calculated from:

$$\bar{T}_2 = \frac{\sum T_i W_i}{\sum W_i} \quad (19)$$

The film temperature drop is determined from the expression:

$$\Delta T_f = \frac{272 D_p^{1.3} G^{.3}}{L [\mu (1-\epsilon)]^{.3}} \quad (20)$$

The ball surface temperature is simply:

$$\bar{T}_s = T + \Delta T_f \quad (21)$$

Finally the temperature in the center of the fuel ball in each matrix cell is obtained from

$$T_c = \bar{T}_s + \frac{75 Q D_p^2}{(1-\epsilon) k} \quad (22)$$

where k , the thermal conductivity of irradiated graphite is given by

$$k = 19.5 \left(\frac{2660 - t}{390.6} \right)^2 \quad (23)$$

where t is the average graphite temperature in the ball and is determined by iteration between equations 22 and 23.

COOLBALL II is also a FORTRANSIT program and therefore all data and results are in the floating point form mentioned earlier.

Table 3.3 lists the card format for input and output to COOLBALL II.

Figure 3.3 shows the calculation flowsheet for this program.

Table 3.4 lists the running deck in standard seven-per-card format. The word -01(LOC)8000 is listed in all unused drum positions.

Figure 3.4 indicates the operating instructions for COOLBALL II.

TABLE 1.1
CARD FORMAT COOLBALL PART II

Card	Word 1	Word 2	Word 3	INPUT Word 4	Word 5	Word 6	Word 7	CC73
1	Identification	MW*	T_{in}	P	W	A	ΔL_1	+
2	ΔL_2	ΔL_3	ΔL_4	ΔL_5	ΔL_6	ΔL_7	ΔL_8	+
3	ΔL_9	ΔL_{10}	ΔL_{11}	ΔL_{12}	ΔL_{13}	ΔL_{14}	ΔL_{15}	+
4	ΔL_{16}	ΔL_{17}	ΔL_{18}	ΔL_{19}	ΔL_{20}	+	NMU	+
5	\bar{T}	blank	blank	blank	blank	blank	blank	+
6	\bar{C}_p	CpX	+	c 1	c 2	c 3	c 4	+
7	c 5	c 6	c 7	c 8	c 9	c 10	c 11	+
8	c 12	c 13	c 14	c 15	c 16	c 17	c 18	+
9	c 19	c 20	D _p	J*	\bar{Pr}	PrX	I*	+
10	A ₁	A ₂	A ₃	A ₄	A ₅	A ₆	A ₇	+
11	A ₈	A ₉	A ₁₀	A ₁₁	A ₁₂	A ₁₃	A ₁₄	+
12	A ₁₅	A ₁₆	A ₁₇	A ₁₈	A ₁₉	A ₂₀	blank	+
13-72	COOLBALL Part I							
	* Fixed point number							

Card	Word 1	Word 2	Word 3	OUTPUT Word 4	Word 5	Word 6	Word 7	Word 8
1	Identification	MW	T_{in}	P	W	\bar{G}	blank	blank
2	P _j	J	blank	blank	blank	blank	blank	blank
3	\bar{T}_2	T _{*1,1}	T _{*2,1}	T _{*3,1}	T _{*4,1}	T _{*5,1}	T _{*6,1}	blank
4	T _{*7,1}	T _{*8,1}	T _{*9,1}	T _{*10,1}	T _{*11,1}	T _{*12,1}	T _{*13,1}	blank
5	T _{*14,1}	T _{*15,1}	T _{*16,1}	T _{*17,1}	T _{*18,1}	T _{*19,1}	T _{*20,1}	blank
6	T _{1,1}	T _{2,1}	T _{3,1}	T _{4,1}	T _{5,1}	T _{6,1}	T _{7,1}	blank
7	T _{8,1}	T _{9,1}	T _{10,1}	T _{11,1}	T _{12,1}	T _{13,1}	T _{14,1}	blank
8	T _{15,1}	T _{16,1}	T _{17,1}	T _{18,1}	T _{19,1}	T _{20,1}	T _{b1,1}	blank
9	T _{b2,1}	T _{b3,1}	T _{b4,1}	T _{b5,1}	T _{b6,1}	T _{b7,1}	T _{b8,1}	blank
10	T _{b9,1}	T _{b10,1}	T _{b11,1}	T _{b12,1}	T _{b13,1}	T _{b14,1}	T _{b15,1}	blank
11	T _{b16,1}	T _{b17,1}	T _{b18,1}	T _{b19,1}	T _{b20,1}	G _{1,1}	G _{2,1}	blank
12	G _{3,1}	G _{4,1}	G _{5,1}	G _{6,1}	G _{7,1}	G _{8,1}	G _{9,1}	blank
13	G _{10,1}	G _{11,1}	G _{12,1}	G _{13,1}	G _{14,1}	G _{15,1}	G _{16,1}	blank
14	G _{17,1}	G _{18,1}	G _{19,1}	G _{20,1}	blank	blank	blank	blank

Cards 2 through 14 repeated for each axial layer

TABLE 3.4
COOLBALL II PROGRAM LISTING IN SEVEN-PER-CARD FORM

```

00000001 109446468554 7011900400000 80000 6911955219555 6911955 10558 1055100
00000002 1119446468554 7011900400000 80000 6911955219555 6911955 10558 1055100
00000003 101199887119991 10119994400003 108000119855 241198519006 241199955 10558 1055100
00000004 151199887119991 10119994400003 108000119855 241198519006 241199955 10558 1055100
00000005 6911955219555 158000180003 6911955219555 241198519006 241199955 10558 1055100
00000006 500000 20119668004771 107266926654 109933649554 109954974554 10948850554 10967375554
00000007 7113998 1094646468554 109003800754 108300018554 10764911554 107233566554 10558 105513554
00000008 105580890854 20534948554 104593369554 10387555554 102933878554 10451310554 103344476554 10090118554
00000009 959099888553 992202475553 884750013553 8220000000553 755972550553 71268858553 607535550553 6054118553
00000010 54317073353 4495975153 462235074552 47422100552 375461119553 47085034552 48123383052 46953633552 445672552
00000011 40678734552 362808472552 35808472552 345024508552 106648142552 22660040552 22660040552 26568515552 24012870552
00000012 1982290140552 158853120552 62600614551 62600614551 100599880000 100599880000 100599880000 100599880000 7998875551
00000013 64099325051 62600614551 62600614551 74750649551 60022921751 600633934551 600633934551 600633934551 6114939551
00000014 7019999999999 62600614551 62600614551 62600614551 62600614551 62600614551 62600614551 62600614551 62600614551
00000015 8419999999999 62600614551 62600614551 62600614551 62600614551 62600614551 62600614551 62600614551 62600614551
00000016 9911999999999 62600614551 62600614551 62600614551 62600614551 62600614551 62600614551 62600614551 62600614551
00000017 1099819999999 81202886951 747552459551 75031668550 7508438150 7519231450 7643981150 7803928150 7959798550
00000018 1122199999999 93453152550 936866456550 936866456550 7962339550 7902174350 79229880850 8275948050 8275948050
00000019 1191999999999 1011980000 1012080000 1012080000 1012080000 1012080000 1012080000 1012080000 1012080000
00000020 1136199999999 10283338352 10283338352 10283338352 10283338352 10283338352 10283338352 10283338352 10283338352
00000021 1171999999999 68048666551 937500000551 95487665451 95487665451 95487665451 95487665451 95487665451 95487665451
00000022 1401999999999 6100000050 6100000050 60700000050 60200000050 60200000050 60200000050 60200000050 60200000050
00000023 1454199999999 6000000050 60200000050 60200000050 60200000050 60200000050 60200000050 60200000050 60200000050
00000024 1611999999999 1016180000 222535688550 198609915550 198609915550 198609915550 198609915550 198609915550 198609915550
00000025 1681999999999 1912128863550 192293858550 195180918550 195180918550 195180918550 195180918550 195180918550 195180918550
00000026 1751999999999 196128840550 196236776550 20121879550 20121879550 20121879550 20121879550 20121879550 20121879550
00000027 1821999999999 2400000050 72100000050 10920000051 10920000051 10920000051 10920000051 10920000051 10920000051
00000028 1891999999999 43950000051 24340000051 19940000051 19940000051 19940000051 19940000051 19940000051 19940000051
00000029 1961999999999 81200000051 27900000051 33620000051 33620000051 33620000051 33620000051 33620000051 33620000051
00000030 2031999999999 1070252354 1071786454 1071786454 1044927354 1044927354 1072675654 1071170054 1068097054 1062780054
00000031 2171999999999 1058086854 1055105254 1055105254 1044927354 1044927354 1072675654 1044804854 1041485354 1036022454
00000032 2241999999999 103308299054 1024050054 1024050054 1044927354 1044927354 1275000051 1427000051 1616000051 1616000051 3720000051
00000033 2311999999999 12319331154 1222257754 1230053254 1230053254 1230053254 1230053254 1230053254 1230053254 1230053254 1230053254 1230053254
00000034 2341999999999 1173119254 1148570954 1128022054 1128022054 1128022054 1128022054 1128022054 1128022054 1128022054 1128022054 1128022054
00000035 2381999999999 1068533554 4100000050 4100000050 4100000050 4100000050 4100000050 4100000050 4100000050 4100000050 4100000050 4100000050
00000036 4551999999999 4100000050 4100000050 4100000050 4100000050 4100000050 4100000050 4100000050 4100000050 4100000050 4100000050 4100000050

```


TABLE 3.4 (cont.)

5601996	6503391193	2000000553	6500021058	6910661852	1110671423	1505680723	6919671026
5671996	1509700875	2402010554	6503001256	6503061361	6503000955	6502970401	6900008002
5741996	6503560661	2000000654	6502830587	1502981412	2019661319	2019700373	2019661019
5811996		6603100416	650100022	1058480000	2019720525	1058668000	6904401801
5881996	1058880000	6680020697	1059080000		1059280000	1059380000	1089480000
5951996	4904981902	1059680000	2000000051	1059880000	1059980000	1060080000	
6021996	1060280000	6503000605	6503000803	35000040515	6504090313	3000000050	6519671571
6091996	6504120767	35000041126	20000000603		6501410745	6680021073	1506180773
6161996	20000000860	1510208002	24000010604	6503001307	6503001555	1180011528	6502900545
6231996	6900008002	6503001005	6919680521	2019690572	2445000048	6507310885	200121
6301996	6503001060	6903841802	1063280000	2019690482	1063480000	2019660569	1063680000
6371996	1063780000	1063880000	1063980000	1064080000	20000000659	1064280000	6506270631
6441996	1064480000	2000001503	1064680000	2019660719	1064880000	1064980000	1065080000
6511996	1065180000	1065280000	6503000655	6504570761	35000040565	6502910595	6502890893
6581996	6519660922	6507631218	35000041176	20000000653	69000210226	2006380671	6519691173
6651996	1506688002	2003111164	1510708002	6601210575	2019681521	6500010756	6907240928
6721996	2400001353	6900008002	6502990953	6905281800	6502900445	6905301802	6507810935
6791996	6503820437	2402211127	6904841907	1068280000	2019700423	1068480000	2000000608
6861996	1068680000	1068780000	1068880000	1068980000	20000000911	1069080000	1069280000
6931996	1069380000	1069480000	2000001354	1069580000	20000000911	1069680000	1069780000
7001996	1070080000	1070180000	1070280000	6680020711	6503000456	2003000703	35000040367
7071996	20000021255	6503000758	6911251902	2019661419	1504140319	6502850439	6911161902
7141996	2019660419	1507180823	6903110766	15112000925	2401410394	6502980508	2402011454
7211996	6908761852	6506381028	6900008002	3500000053	2000001553	2019670570	2000000658
7281996	6508310985	600001	6500410995	2000001	1073280000	6903361907	1073480000
7351996	2000000808	1073680000	1073780000	1073880000	1073980000	1074080000	1074180000
7421996	1074280000	2000001004	1074480000	6903481800	1074680000	6503000863	1074880000
7491996	1074980000	1075080000	1075180000	1075280000	6502840389	6503001258	35000040615
7561996	2000001404	5000000050	3500040869	6519661372	35000041226	6904641852	5
7631996	2000000052	6519660921	1507688002	2400001462	2019681421	6501210625	1508228002
7701996	6503000856	4609781130	6680020981	6900008002	2019660369	6900008002	6919670920
7771996	6900008002	6508821035	6904321913	6500011210	200221	1078280000	2019691524
7841996	1078480000	6900008002	1078680000	1078780000	1078880000	1078980000	1079080000
7911996	1079180000	1079280000	6903961802	1079480000	2000000759	1079680000	1079780000
7981996	1079880000	1079980000	1080080000	1080180000	1080280000	6503000755	6915781587
8051996	3500040665	3500040417	6908571802	6503000858	6908621902	3500041326	1502981103
8121996	3500041523	6907471852	6504571311	1508188002	6514651519	1511708002	6501410345
8191996	1508728002	6502010906	6907741800	6600611515	6900008002	6502910495	2000001006
8261996	24000000754	6905801802	1502950499	6904821907	6503001310	310	1083280000
8331996	6900008002	1083480000	6900008002	1083680000	1083780000	1083880000	1083980000
8401996	1084080000	1084180000	1084280000	2000001204	1084480000	2000000909	1084680000
8471996	1084780000	1084880000	1084980000	1085080000	1085180000	1085280000	6905711950
8541996	6505570961	3500040715	3500040467	2019681321	3500040919	6502850489	6519691376
8611996	1086180000	2003100363	1509668002	2003050408	1508680923	6913240872	1512208002

TABLE 3.4 (cont.)

85811996	2401210674	15097288002	6501210825	6908241902	6500810685	1270000051	6502920497
87511996	69000008002	65142290883	20000001508	2403001213	6905321907	2400011114	400003
88211996	1088280000	69038618000	1088480000	-2019690678	1088680000	1088780000	1088880000
88911996	1088980000	10890780000	1089180000	-1089280000	20000001304	1089480000	6919671425
89611996	1089680000	10897780000	1089880000	-1089980000	10900080000	1090180000	1090280000
90311996	6915361590	6502960331	35000040765	20000001504	65030009557	20030009558	6502850539
91011996	35000041476	6512141069	4604660516	1511661172	6503391043	1509180973	1715781535
91711996	1512700975	2400610514	1510220777	24000001056	6908741852	6910251852	6900008002
92411996	100033	69000008002	6502410795	2019681572	24000001554	6905821907	69000011460
93111996	20063990772	10932680000	6880020641	1093480000	2019700728	1093680000	1093780000
93811996	1093880000	1093980000	1094080000	-1094180000	1094280000	2003060459	1094480000
94511996	2019691276	1094680000	1094780000	-1094880000	1094980000	1095080000	1095180000
95211996	1095280000	20000001003	2019670420	35000040815	35000040517	35000040817	6680020967
95911996	66022211075	6519681576	2000000904	2019661219	20030001113	2003070510	1509688002
96611996	65022211078	1502981008	65000011355	1096980000	-2401011156	6509240779	6500810735
97311996	69000008002	65030001305	69000008002	6500610566	20012	6906391072	2019671575
98011996	6502611560	20000000410	1098280000	-1098380000	1098480000	2019710778	1098680000
98711996	1098780000	1098880000	1098980000	-1099080000	1099180000	1099280000	20030001253
99411996	1099480000	2019661469	1099680000	-1099780000	1099880000	1099980000	1100080000
100111996	1100180000	1100280000	65030001055	6506071011	35000040865	6501220677	6503071511
100811996	4605620708	6906631902	6904131902	6906141902	20196671325	6680021322	6503391343
101511996	1510188002	1101680000	6915201950	6500611055	6512220877	6501810635	6503001405
102211996	2400611014	2000000406	6502410645	2003080512	24000001509	6906301852	6909311802
102911996	6503021559	1103080000	1103180000	-1103280000	1103380000	1103480000	6904381907
103611996	1103680000	1103780000	1103880000	-1103980000	1104080000	1104180000	1104280000
104311996	1503001456	1104480000	1503061562	1104680000	1104780000	1104880000	1104980000
105011996	1105080000	1105180000	1105280000	-6680020811	6505571061	35000040915	6905591950
105711996	20030001107	200000021108	6503031109	35000041077	6906641902	6519661475	4608160704
106411996	6503000660	20000001403	2006371420	24000810564	6500210725	6907221852	6501011306
107111996	1510248002	2407240671	20000001153	20196660469	20000000404	6910291902	1506800785
107811996	6910811852	2401611064	6909331852	6503000913	1108280000	1108380000	1108480000
108511996	1108580000	1108680000	1108780000	-1108880000	1108980000	1109080000	1109180000
109211996	1109280000	2003000907	1109480000	-1005481163	1109680000	1109780000	1109880000
109911996	1109980000	1110080000	1110180000	-1110280000	4605060753	6502880793	20030001053
110611996	35000040567	6680021365	7120432	2019671574	35000041177	2019670470	6519661076
111311996	30000041013	65030001410	1510688002	6680021023	1111780000	2400410444	6503060812
112011996	2402610914	6910741800	24000000813	6906261852	65030001505	2019661119	1510790833
112711996	6503001110	1010671163	6502010710	6506391122	2006010704	1113280000	1113380000
113411996	1113480000	1113580000	1113680000	-1113780000	1113880000	1113980000	1114080000
114111996	1114180000	1114280000	15030001057	-1114480000	1114580000	1114680000	1114780000
114811996	1114880000	1114980000	1115080000	-1115180000	1115280000	6519691123	6605571161
115511996	6903581902	65030001206	4605600907	2660000054	35000041169	35000041227	6907141902
116211996	6503000610	1013241230	6503391543	1511181273	2400611264	1116780000	6500410695
116911996	1512258002	6502611315	6911241902	69000008002	6906761652	2019660519	6503010809

TABLE 3.4 (cont.)

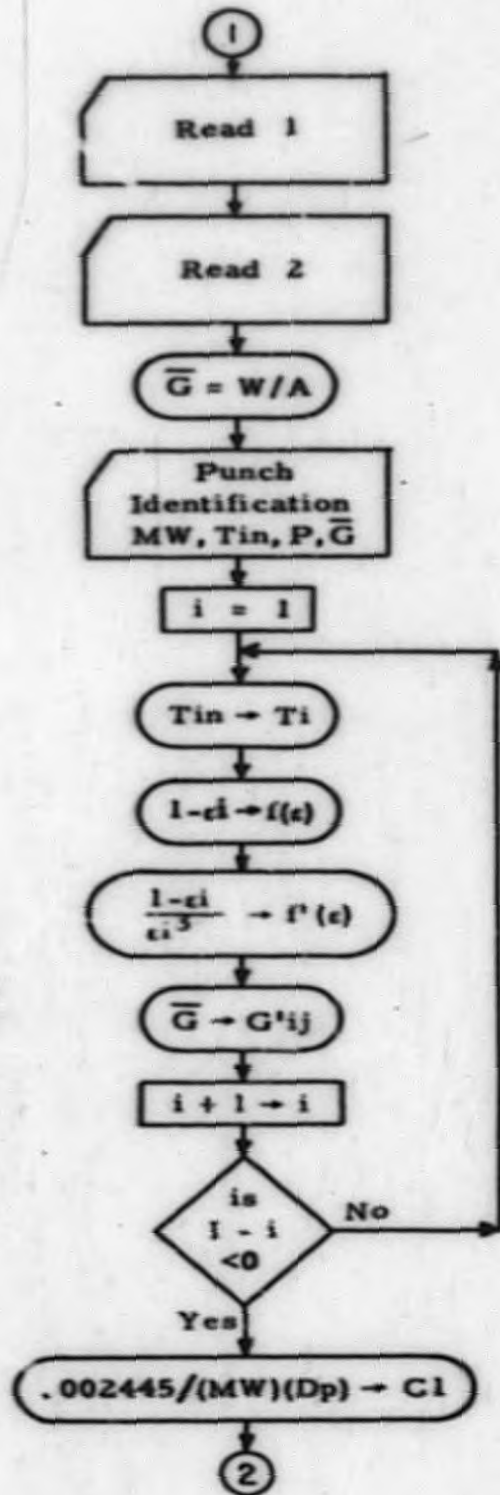
11761996	15112980002	15073308002	69111311902	6501410945	1503000963	1118180000	1118280000
11831996	1118380000	1118480000	1118580000	1118680000	1118780000	1118880000	1118980000
11901996	1119080000	1119180000	1119280000	2003001207	1119480000	1119580000	1119680000
11971996	1119780000	1119880000	1119980000	1120080000	1120180000	1120280000	6905561950
12041996	6506071211	6502970501	35000040617	6503071561	1506628002	6919671275	2000001260
12111996	6907641902	2403111059	6502940549	1915000052	1511688002	6515691178	1121780000
12181996	6907711852	6506071012	6501011357	6911741800	2000000051	6907261902	6503000806
12251996	6502011209	1511798002	1507808002	1122880000	6501610616	1513248002	1123180000
12321996	1123280000	1123380000	1123480000	1123580000	1123680000	1123780000	1123880000
12391996	1123980000	1124080000	1124180000	1124280000	15030001507	1124480000	1124580000
12461996	1124680000	1124780000	1124880000	1124980000	1125080000	1125180000	1125280000
12531996	6502920547	6502940449	6503390993	3500040667	6502860441	1506138002	6909621950
12601996	6519661277	6908141902	6503111527	6912161902	6513241180	1502981556	1126660000
12671996	1126780000	1126880000	1513758002	2400810434	6912241852	6915581902	69000008002
12741996	6503001406	24000001259	6503000810	6908301852	1127880000	2019681426	1128080000
12811996	1128180000	1128280000	1128380000	1128480000	1128580000	1128680000	1128780000
12881996	1128880000	1128980000	1129080000	1129180000	1129280000	2003000708	1129480000
12951996	1129530000	1129680000	1129780000	1129880000	1129980000	1130080000	1130180000
13021996	1130280000	6519710675	6505071261	3500040965	20000001356	3500040867	5200000050
13091996	3500041269	3500041327	6908641852	2003001362	1131380000	1131480000	2000001007
13161996	1131680000	1131780000	1131880000	6515250979	6502980558	6503000956	1502981063
13231996	6907761902	100000	6503001309	1512298002	1508800835	1132880000	6500211526
13301996	1133080000	1133180000	1133280000	1133380000	1133480000	1133580000	1133680000
13371996	1133780000	1133880000	1133980000	1134080000	1134180000	1134280000	1503000908
13441996	1134480000	1134580000	1134680000	1134780000	1134880000	1134980000	1135080000
13511996	1135180000	1135280000	6906561950	6519671221	20000001303	6519661371	2000001407
13581996	1107621517	6910621950	6903551212	3500041071	66800020577	1136380000	1136480000
13651996	1502981157	1136680000	1136780000	1136880000	1509768002	1474	6912741902
13721996	6911751902	1137380000	6503001457	6501410895	6912791902	1509308002	1137880000
13791996	6503041010	1138080000	1138180000	1138280000	1138380000	1138480000	1138580000
13861996	1138680000	1138780000	1138880000	1138980000	1139080000	1139180000	1139280000
13931996	1139380000	1139480000	1139580000	1139680000	1139780000	1139880000	1139980000
14001996	1140080000	1140180000	1140280000	6519681223	6519661271	3500041015	3500040717
14071996	6519661471	6501220827	3500041369	3500041377	2019670770	4607161059	1141380000
14141996	1141480000	1502980458	1141680000	1141780000	1141880000	6503000760	6503001208
14211996	6513240829	2019681472	4411280388	6907270354	24000001359	6503000910	6503001510
14281996	1142880000	3906405053	1143080000	1143180000	1143280000	1143380000	1143480000
14351996	1143580000	1143680000	1143780000	1143880000	1143980000	1144080000	1144180000
14421996	1144280000	1144380000	1144480000	1144580000	1144680000	1144780000	1144880000
14491996	1144980000	2416091681	1145180000	1145280000	2416061759	6507571411	3500041115
14561996	2003001506	3500040917	6916111453	3500081486	24000001427	2003070460	6503070541
14631996	1146380000	1146480000	400061	1146680000	30000071681	1146880000	6503001160
14701996	1147080000	6913741902	6513240929	3100031483	6503391293	6905781902	1513298002
14771996	1509808002	2019331488	1147980000	1148080000	1148180000	1148280000	6087021491

TABLE 3.4 (cont.)

14841996	1148480000	1148580000	2019911494	1148780000	6819911645	1148980000	1149080000
14911996	1919441467	1149280000	20030001360	16800011856	1149580000	1149680000	1149780000
14981996	1149880000	1149980000	22415791532	16800020509	300000615667	6519671121	6502020807
15051996	3500041165	6680021265	20030001557	65000621017	6911121950	3500041477	6909641852
15121996	2000161	1151380000	1151480000	2019671320	1151680000	4406211372	1151880000
15191996	2019680628	6519661272	6513240879	114714714	1151980000	6509770681	7000000050
15261996	200000009650	69066661852	4415881372	1152980000	22215361589	2015811534	69800001538
15331996	7115770527	2115801533	6915771530	16800021545	2415781531	3000051501	3000051501
15401996	6915791541	1154280000	1154280000	1503001312	22215481551	1715480804	1154680000
15471996	1154780000	90315550	2215771537	2415791577	30000031358	2415411588	6519661171
15541996	6513080713	35000041215	4606091253	6680021415	6502020709	6911621902	6918621902
15611996	20000001257	200030060463	1156380000	1156480000	1156580000	1156680000	1006121568
15681996	1515811540	7500000052	6515730927	6914241852	6504290783	305	6503001159
15751996	6503001409	6913791800	5980001538	1157880000	1157980000	1158080000	1158180000
15821996	1158280000	1158380000	1158480000	1158580000	1158680000	2315411544	3000051502
15891996	35000041549	2415771591	6915791577	1159280000	1159380000	1159480000	1159580000
15961996	1159680000	1159780000	1159880000	1159980000	2416051458	1	2416051459
16031996	6502910595	2000001605	6919670920	2416091681	31000091478	1000000051	7000000000
16101996	6914501453	2416091473	1161280000	4416221842	2419221675	4516771940	2019851788
16171996	24000011922	6519251631	2019251733	1080031640	2219251833	30000011932	4417271938
16241996	35000071743	1002080001	6519111669	20193311699	1118311703	2019841638	1519331887
16311996	4516361916	4416861694	4516911696	1019391644	2016081811	1619391619	6500001605
16381996	6019911695	35000021998	1619931749	20000001704	1647	2419161668	2119981618
16451996	1519481736	1516091813	7019521997	6919528002	6919538002	6919548002	6919558002
16521996	6919568002	1119651934	6516121963	2019911848	6780021915	6919321985	3500081716
16591996	3000021683	20193311841	1618171821	6919171824	1000018001	6900018003	4417251692
16661996	1050018001	6419221842	6917221851	4616541928	6517301988	3000051731	1619251630
16731996	6019311888	6018311748	6916791682	6580031992	6719311693	6519331639	1519391793
16801996	4418831737	6919371643	2319851618	6419911879	6500001755	1516178003	1119391694
16871996	2019911894	6519911895	6916421945	4519191996	6917461901	6000001705	1619171871
16941996	1019981911	1519531909	6600001814	2416091757	6019981912	6016081665	6919031606
17011996	6080031859	2416051658	6419251847	6719111633	4417171735	2019111684	1080011663
17081996	3500081768	2119161920	2119161789	4416731699	69193311740	6980031621	1518171771
17151996	6919241880	2119331738	4617351928	1918261857	6980031947	2419851878	3500041632
17221996	20193311605	1619851889	3000041834	6019911845	6519291722	66193311992	2019331786
17291996	3000041835	1516648002	2219851739	6880021742	1517968002	6919901844	6519911615
17361996	6880021645	6917411671	6880021798	4517091797	24000001858	3500001807	1519951899
17431996	2019981809	3500081772	3100011751	6919641902	6916051663	2116041764	2016091812
17501996	2416031994	6416041875	2416051791	3000081867	6519331787	2416121938	4619491661
17571996	4518601604	4617231773	4617471763	1019141748	4617141923	1080011721	3500081620
17641996	6019251930	6019311785	1418261770	2319251878	2119331736	2419221935	2119251830
17711996	4619431825	2016091674	1519851889	2419771922	2419781922	2419791922	2419801922
17781996	2419811922	2419821922	2419831836	4616341985	1519851790	2016091862	6019911898
17851996	3000011667	1519911655	3500041998	6019911822	6919931697	1580011700	6918951801

TABLE 3.4 (cont.)

17921996	6019981758	7119771629	100508001	1980011829	6019681739	2116091869	1519061761
17991996	2019531921	2416051660	2416041710	2416051858	1119061718	2416081662	1916081946
18061996	1019141681	1580011613	6918161872	6519171672	6918661872	6019141822	6019221828
18131996	1719161871	4616761940	1019171935	6780021783	1000000000	1618271782	2119251628
18201996	1419271853	4617241726	1018311886	3500011680	2419311837	3000041734	2302585093
18271996	6931471806	1919311842	3100101635	2419331936	2000000000	1519851616	1680011690
18341996	1519891843	1180031849	2119911799	2019911896	6080011795	3600001767	4418931949
18411996	6500001712	6918951851	2019981754	2219981678	1980011837	6016011805	2015011720
18481996	6016041760	3000061762	2416031706	2416041757	2416051808	2016081711	2019161870
18551996	2416081861	1918261607	3000071818	6918641872	1019141819	4417151865	3000021868
18621996	1819161823	6980028003	4417321949	6080021874	6780021640	4516241672	2119221925
18691996	6519221877	2119311890	4619491876	2419251667	4516761928	6919271880	4517281784
18761996	4419491881	6919311985	6580031885	4518321884	2419331839	2019851793	6516851689
18831996	4616881637	6019981803	3100021892	2119911846	3500081646	1919911627	3000081604
18901996	6000001855	1119261781	2019981753	2019981701	3500081854	2000001605	6716081820
18971996	4517071960	3000011806	2016091765	2416051708	2416051610	2416051810	807000000
19041996	2019111918	4619191960	5000000000	2419601713	2319841941	1119651922	2419161670
19111996	7887445650	6918151769	2419161719	1000000000	2019111633	5100000000	1
19181996	6918911614	6919841908	6519311657	6519841679	1000000000	6580031895	12
19251996	5	9999	9999	6519311992	10000000051	1919331743	100000000
19321996	3500011842	12	6919578002	1119421897	2419911744	4000000000	6916411801
19391996	10000	6916031625	6916981910	1774	6916051666	4342944819	2419981904
19461996	2116011659	2219251882	5200000000	6916051794	2416031656	20013	6500181994
19611996	119618000	119628000	1419271623	6916261900	7	2033936752	5000000050
19681996	1000000051	200221	200221	1360000054	282	281	200121
19751996	292	291	8120286951	2419821999	2419831958	2419848000	6919541957
80001997	5100000000	8008	100000000	2419851999	2419861958	2419878000	6919541957
80001997	6919421945	3100111766	30999991895	2419881999	2419891958	2419908000	6919541957
80001997	1000000051	2000001603	5800000000	2419911999	2419921958	2419938000	6919541957
80001997	6900001804	4900000000	1080001905	2419941999	2419951958	2419968000	6919541957
80001998	6919518002	100000000	6504070361	2419971999	2419981958	2419998000	6919541957
1999							



Read 1
 Identification
 MW, T_{in} , P, W
 A, ΔL_j , $\bar{\mu}$, XMU, \bar{T}

Read 2
 \bar{C}_p , C_{pX} , & c_i , D_p
 J, \bar{Pr} , PrX , I, A_i

Calculation Flowsheet
 COOLBALL II

FIG. 3.3
 page 1 of 5

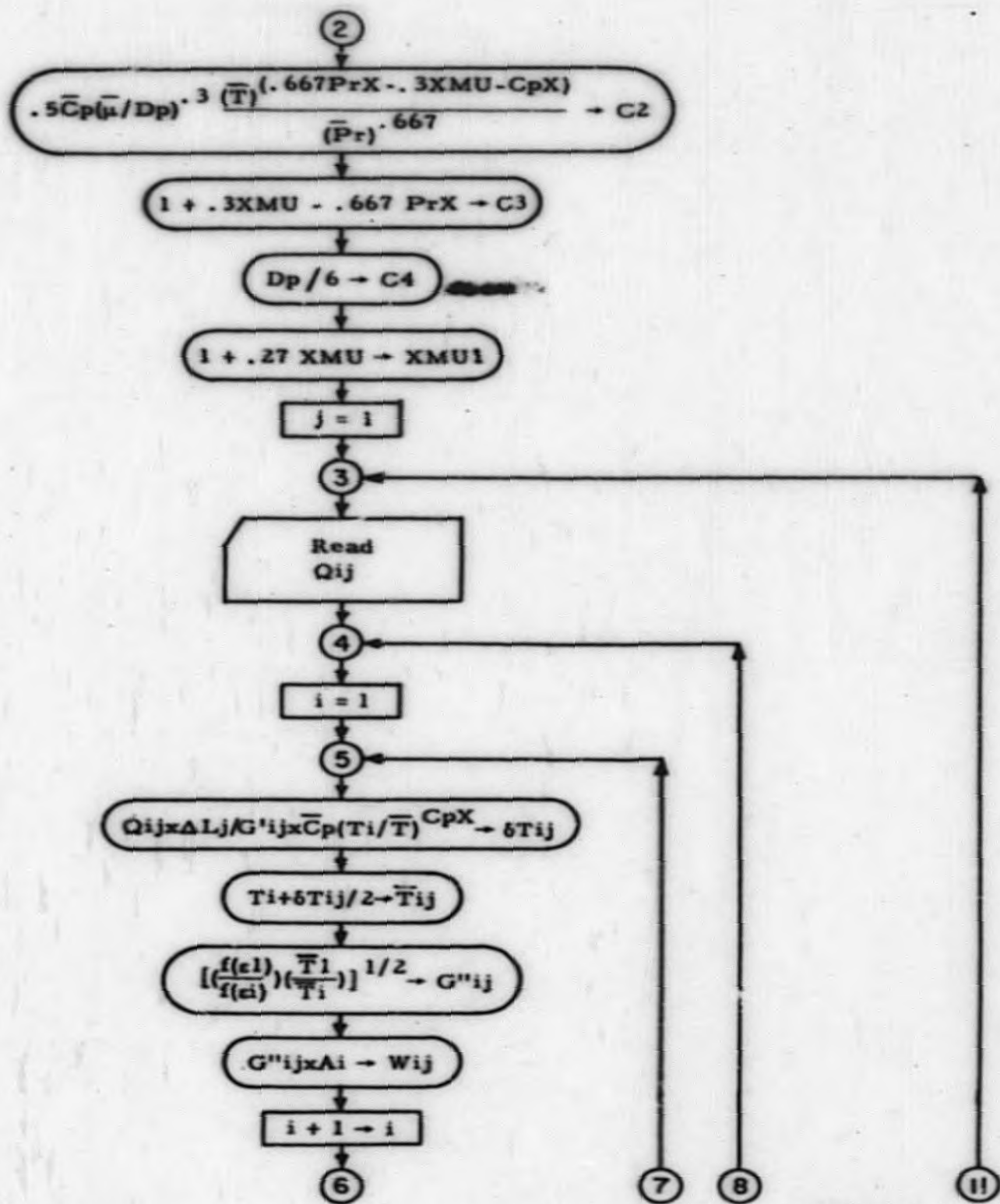


FIG. 3.3
page 2 of 5

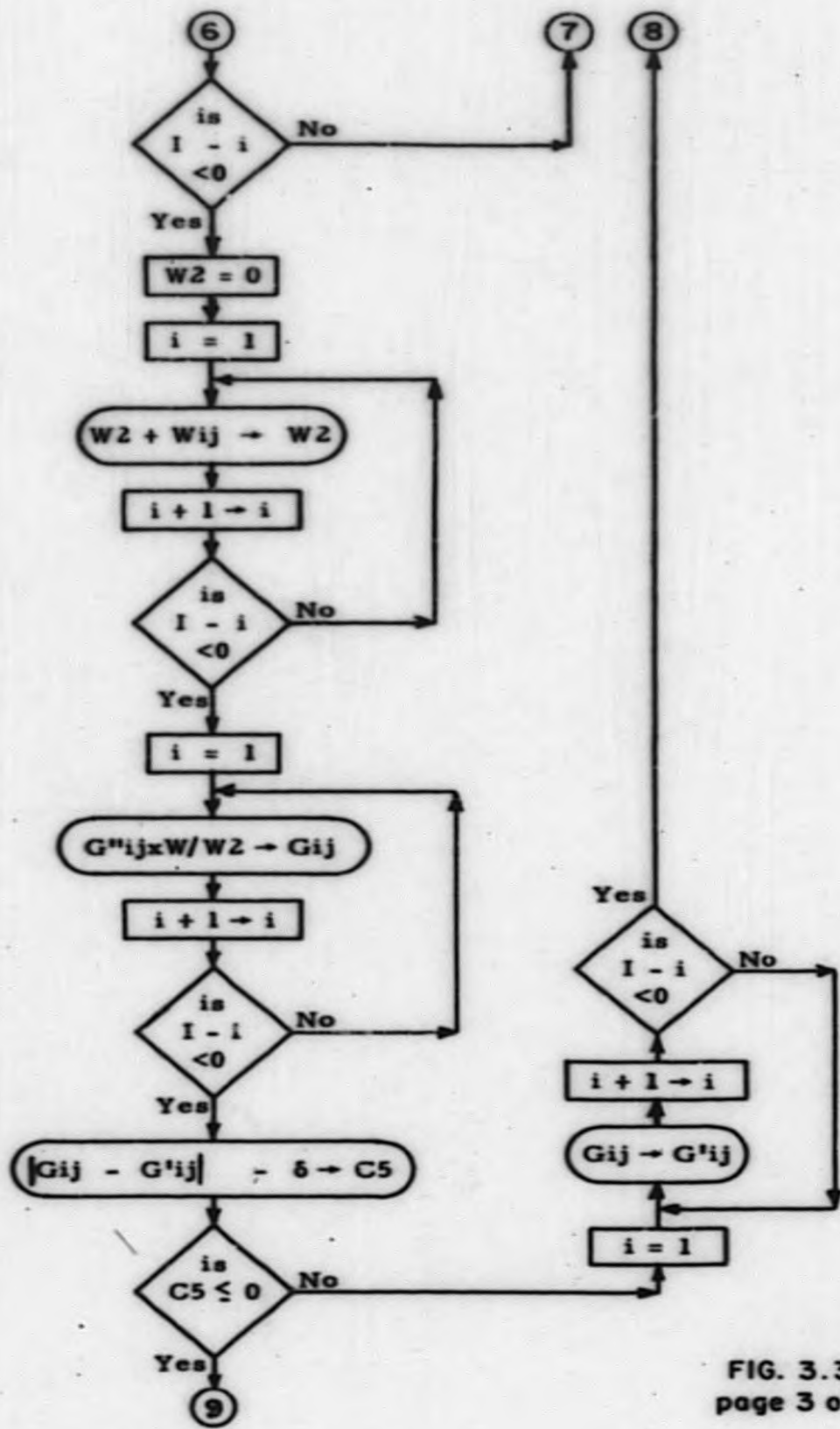


FIG. 3.3
page 3 of 5

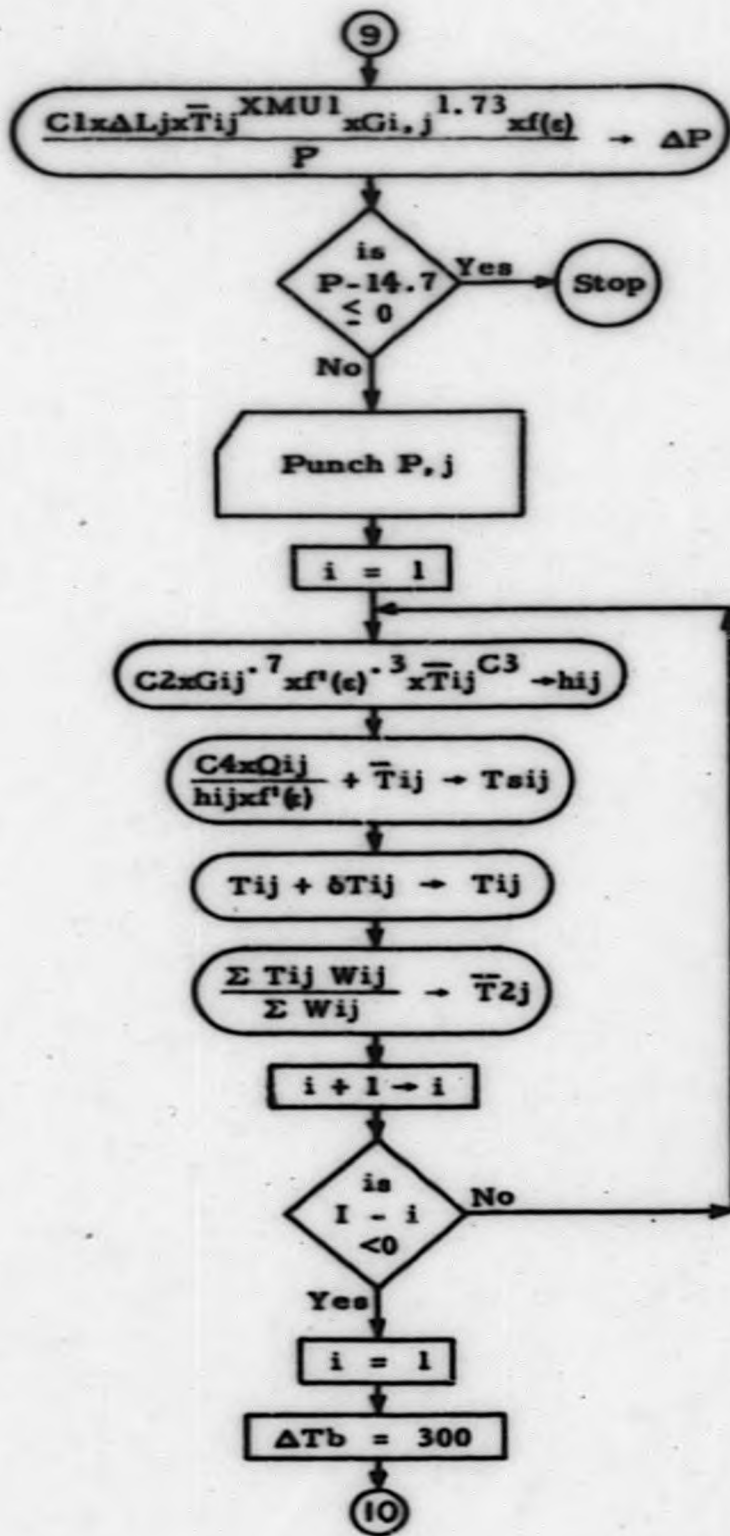


FIG. 3.3
page 4 of 5

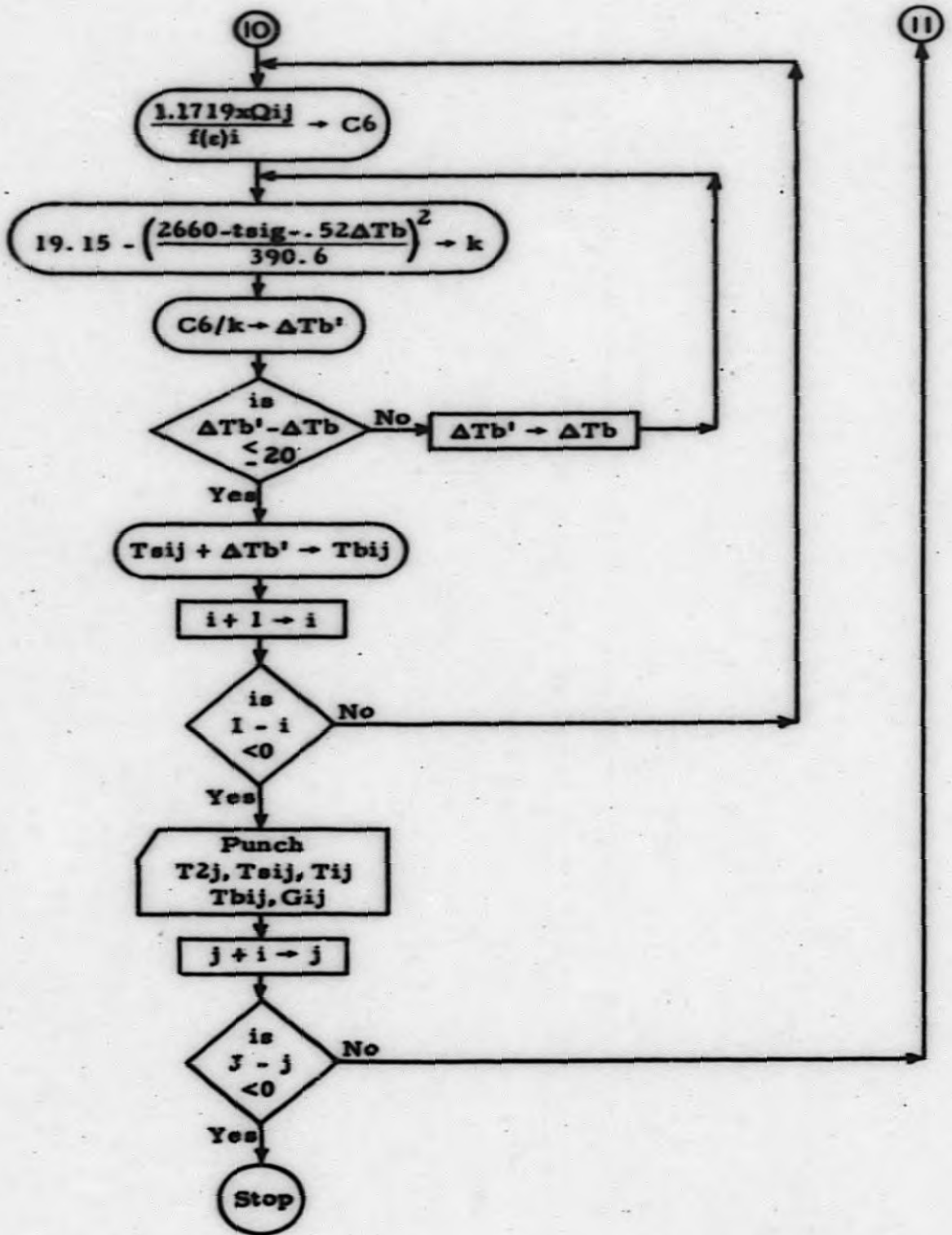


FIG. 3.3
page 5 of 5

Section 4.0 Illustrative Problem

As an illustration of the use of the COOLBALL codes, there is presented the following analysis of a power reactor core of 750 tMW output such as might be used for a large central station power plant. Preliminary analysis of such a Pebble Bed Reactor results in the characteristics indicated in Table 4.1.

TABLE 4.1

Characteristics of 750 tMW Core

Type	Axial Upflow
Core Diameter, ft	17.5
Core Length, ft	14.0
Gas	Helium
Gas Temperature (inlet/outlet), °F	550/1260
Gas Flow, Lbs/sec	755
System pressure, psia	1000
Core Gross Output, tMW	712.5
Core Power Density, MW/Ft ³	.212
Fuel Ball Diameter, inches	3.0

Figure 4.1 shows the assumed radial and axial power profiles (see Ref. 9). A constant voidage of 39% was selected (since the core was surrounded by a reflector of smaller balls and the orienting effect of the wall was negligible). The core region was arbitrarily divided into eleven axial slices and fourteen annular rings, and the average power in each slice and in each ring determined.

Table 4.2 lists the actual input to and output from COOLBALL I. It should be noted that the blank spaces indicated on the third card of the input are actually zeros and are required to fill out the unused radial positions (20 total). In addition, the third output card for each axial slice contains zeros in the first six word positions.

Table 4.3 lists the complete input to and output from COOLBALL II.

TABLE 4.3
COOLBALL II INPUT & OUTPUT FOR 17.5 Ft. Dia. x 14 Ft. 750 MW PEBBLE BED REACTOR

INPUT

1965210001	4	10100000054	10000000054	75500000053	24053000053	70000000050	
14000000051	14000000051	14000000051	14000000051	14000000051	14000000051	14000000051	
14000000051	14000000051	70000000050					
13680000054					24000000046	58000000050	
12500000051		32800000049	39000000050	39000000050	39000000050	39000000050	
39000000050	39000000050	39000000050	39000000050	39000000050	39000000050	39000000050	
39000000050	39000000050	39000000050					
13473000051	39820000051	66366000051	92913000051	11948000052	14599000052	17237000052	
18484000052	20546000052	22808000052	25070000052	27332000052	29594000052	31856000052	
1734699753	1729423953	1705661053	16649522453	1622812053	1564753553	1495648553	10002
1420249553	1339070453	1250608353	1154670553	1059323553	9986832052	1088567353	20002
2337721553	2323013353	2291982053	2243998653	2180653753	2102637653	2009777753	40002
1908460353	1799375953	1680304953	1551588453	1423466053	1341980653	1460074853	50002
2908560553	2891380553	2851652053	2791951753	2713138953	2616072353	2500537453	60002
2374479753	2238758353	2090860753	1930464753	1771056553	1669673553	1816604753	70002
3533765053	3512892253	3464823953	3392090953	3296336953	3178408653	3038036053	80002
2884881953	2719986853	2540298053	2345424453	2151750953	2028575353	2207089953	90002
3615313553	3593959053	3544376753	3470369953	3372406353	3251753453	3108144653	10002
2951458153	2782755753	2598920353	2399549553	2201408753	2075388553	2258022753	11002
3370668753	3350758853	3304718253	3235532953	3144198353	3031710053	2897819053	12002
2751733553	2594448953	2423053553	2237174053	2052439353	1934948753	2105224253	13002
3343485453	3323736553	3278067253	3204439953	3118841953	3007260753	2874449553	14002
2729342153	2573525953	2403512853	2219132353	2035887453	1919344353	2088246553	15002
2799829253	2783291553	2745048253	2687579753	2611713153	2518275253	2407059353	16002
2285714153	2155066453	2012697753	18564697853	1704848853	1607255853	1748694353	17002
2248990353	2215824353	2165378153	2139626653	2079227453	2004840553	1916299753	18002
1819694753	1715684053	1602341853	1479421553	1357258253	1279582953	1392184453	19002
1630968553	1621334953	1599057253	156550453	1521386353	1466956453	1402170553	20002
1331483953	1455378553	1172445253	1089503553	9931157852	9362655052	1018656953	21002
1047312353	1080889953	1066038153	1043720353	1014257553	9779709652	9347803252	22002
8878559852	8269190052	7816301852	7216890352	6620771952	6241770052	6791049852	23002
							33002

OUTPUT

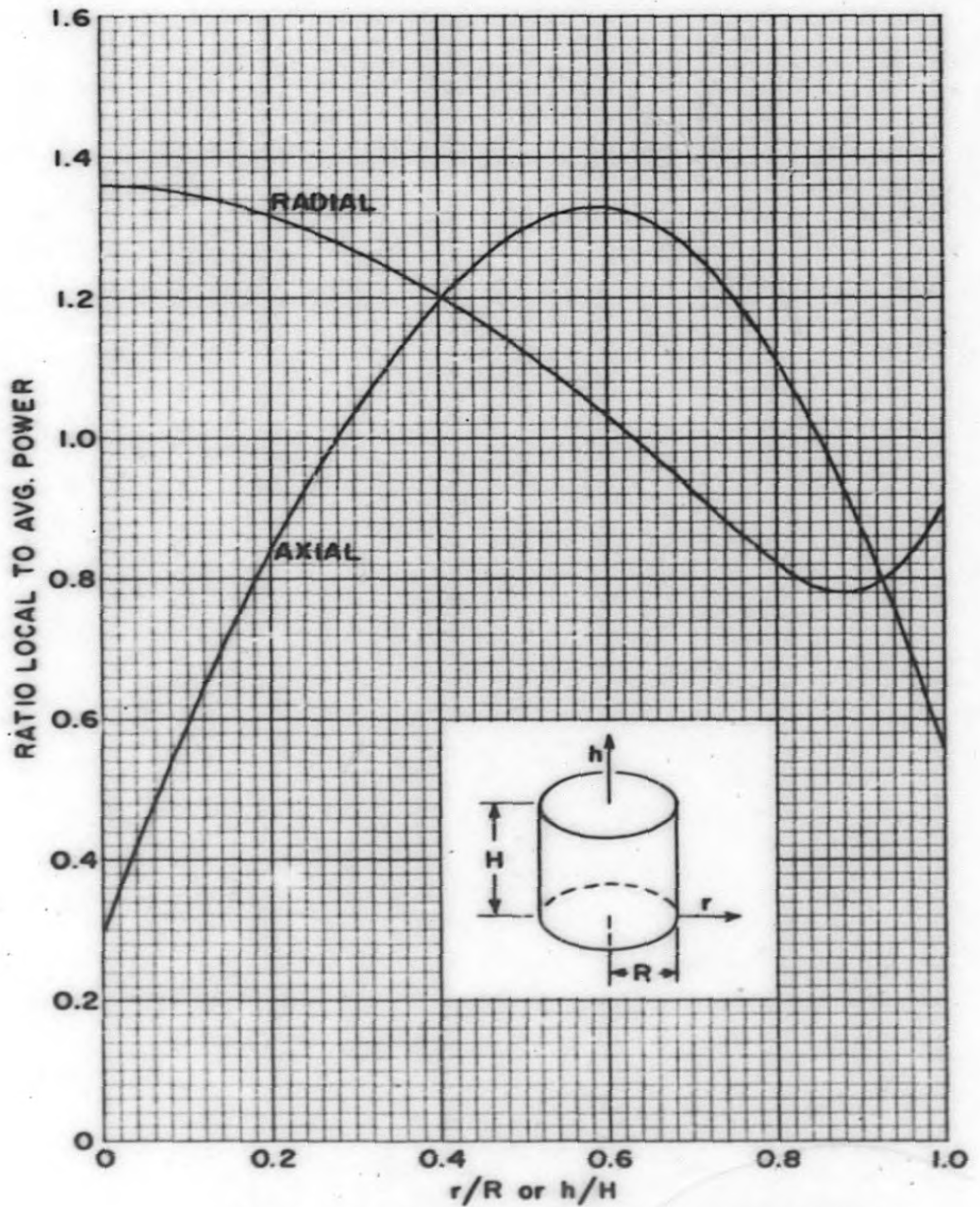
1985410001	4	10100000054	10000000054	75300000053	3138901651	17200001
9998421753	1					17300012
1032851954	1147349154	1146540154	1144669354	1141857754	1138145654	1133572854
1148129054	1122187854	1115789554	1108815354	1101249454	1093727854	1088942854
1098877254						17800003
1041037354	1040854054	1040430154	1039793054	1038952054	1037916254	1036683354
1035338254	1033889954	1032311854	1030600154	1028899054	1027817154	1029389154
						1567941254
1565624854	1560243254	1552089654	1554447954	1540782854	1524150454	1505600454
1485099754	1478851054	1452715654	1425703854	1407939354	1433533354	
						18200003
3133078451	3133565251	3134208451	3135000951	3135944851	3132614551	3132754551
3139299551	3140613851	3141925651	3142759551	3141551251	3136975751	3138087251
						18400003
						18500003
9994331753	2					18800012
1094262254	12455950354	1244539854	1241278854	1236380154	1229916954	1221962454
1217302654	1202191354	1191101354	1179030754	1163958954	1152980654	1144736854
1156688654						18900003
1125204854	1124307754	1122896254	1120476654	1117286154	1113362354	1108700054
1103623454	1098169454	1092240154	1085826454	1079469254	1075435054	1081284054
						1684076954
1681352454	1675026854	1663456554	1663524454	1647600154	1628454754	1607067954
1583490954	1569063154	1539496354	1508973854	1488900554	1517819654	
						3110364851
3112459951	3114661351	3117571851	3121163451	3125448551	3130136851	3135199551
3140734151	3146757051	3152763051	3156597051	3151046251		
						19700003
						19800003
9990601053	3					19900012
1170602354	1378586754	1376347454	1371171354	1363400954	1353156154	1340559454
1325598154	1309307754	1291814554	1272804154	1252248954	1231884054	1218965454
1237898554						20200003
1231043454	1229675754	1226515554	1221774054	1215528254	1207857054	1198756554
1188863354	1178239954	1168733354	1154340354	1142065454	1134291754	1145586354
						1814392254
1811029054	1803234154	1791473354	1775855754	1756465754	1740568754	1714922854
1686664054	1655685054	1621046954	1597195354	1574202954	1607364154	
						3077204551
3081678151	3086385651	3092621651	3100336251	3109568451	3119703251	3130688251
3142745351	3155925251	3169132051	3177588151	3165347351		
						21000003
						21100003
9986375553	4					21200012
1263274054	1536703754	1533442454	1525907154	1514601354	1499708654	1481417254
1459718354	1436134354	1410878354	1383419554	1353821954	1324560654	1306030754
1332905954						21500003
1381155954	1358931054	1353792554	1346088754	1335951654	1323518254	1308793154
1292819054	1275727754	1257230054	1237319054	1217685454	1205278854	1223279754
						1971181054
1966848754	1956823754	1941740554	1921789554	1897145154	1867686154	1841826454

OUTPUT (cont.)

1806957454	1768567054	1726353754	1690369654	1662895554	1702586154		2200003
					3041018451	3043128051	2210003
3048017651	3055394851	3065188451	3077336451	3091921751	3107992651	3125482451	2220003
3144765551	3165946551	3187279551	3200996351	3181154951			2230003
9981824453		5					2240003
1357982954	1671563954	1667382354	1657724554	1643243954	1624186454	1600807754	2250012
1573114054	1543063954	1510904054	1476088454	1438502154	1401627854	1378256254	2260003
1412164154							2270003
1495837054	1492691754	1485430254	1474551054	1460249454	1442729654	1422012054	2280003
1399576054	1375616554	1349739854	1321950354	1294613454	1277377254	1302397254	2290003
						2067787254	2300003
2052634854	2050726754	2032849154	2009274154	1980269454	1943770254	1908127454	2310003
1872199554	1828085554	1780002854	1731630454	1700914054	1745643754		2320003
							2330003
3015106151	3025021651	3038212251	3054616851	3074375751	3096227951	3120105351	2340003
3146547451	3175735351	3205283651	3224363951	3196784751			2350003
9976955353		6					2360003
1446200454	1783282654	1778298054	1766789454	1749544554	1726869054	1699082954	2370003
1668213354	1630803354	1592539254	1551431854	1507284154	1463816454	1438393654	2380012
1476193154							2390003
1622699954	1618660354	1609338154	1593379154	1577043554	1554603054	1528104254	2400003
1499446854	1468892354	1435951054	1400644054	1365986154	1344167554	1375845154	2410003
						2125846754	2420003
2119999754	2106498054	2086259654	2059630954	2026964154	1988250554	1949326754	2430003
1904388454	1855570354	1807717754	1750166854	1716665454	1765192954		2440003
					2975202051	2978635151	2450003
2986605451	2998663051	3014730851	3034759651	3058949851	3085787951	3115216851	2460003
3147932751	3184200451	3221083751	3244949451	3210457851			2470003
9971780453		7					2480003
1533686154	1506068354	14900192554	14886630254	1466318654	1439631054	1406960154	2490003
1768357954	1726594054	1682042054	1633982854	1582440754	1531814454	1499927054	2500003
1546219054							2510012
1749666654	1744709354	1733271854	1716154654	1693686454	1666215854	1633808454	2520003
1598809754	1561546754	1521437354	1478523654	1436478354	1410050854	1448430654	2530003
						2223423654	2540003
2216889054	2201149154	2177885154	2147330954	2109936354	2065748254	2017906654	2550003
1966790554	1911496954	1855320854	1796684254	1759497654	1813413254		2560003
							2570003
2962000951	2975866651	2994371651	3017462451	3045461351	3076588551	3110822951	2580003
3149008651	3191497951	3234878651	3263088451	3222363251			2590003
9966325653		8					2600003
1606839854	1985685154	1979181854	1964175854	1941713354	1912221054	1876149554	2610003
1833377254	1787577754	1738577854	1685803954	1629305254	1573914054	1539079954	2620003
1589663854							2630003
							2640012
							2650003
							2660003
							2670003

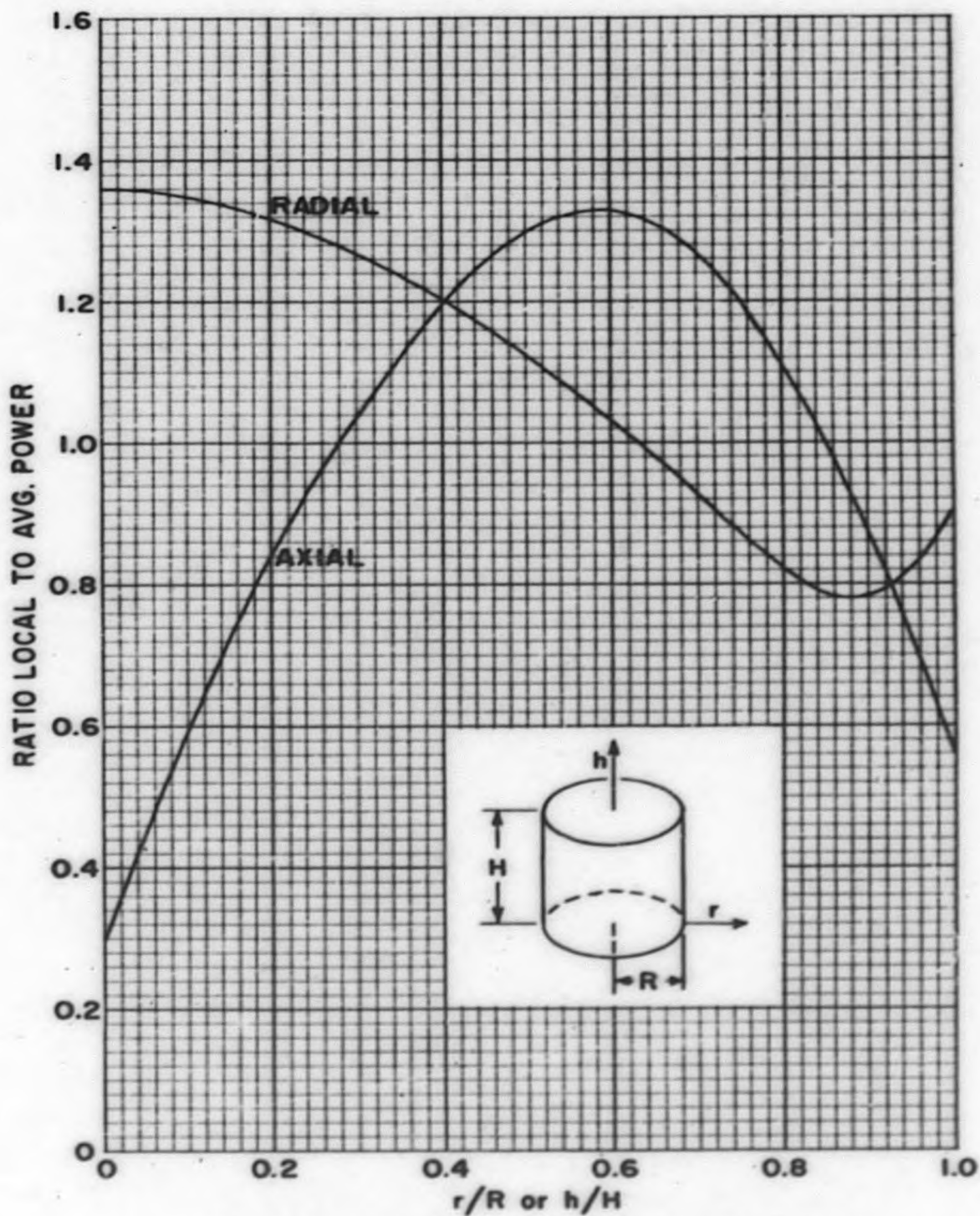
OUTPUT (cont.)

1856786554	1851038654	1837780054	1817945054	1791923754	1760131154	1722657454	2680003
1682227154	1639230054	1593004854	1543615554	1495296654	1464963154	1509025054	2690003
2235239854	2218567154	2193627454	2160910654	2120930354	2073778354	2022847354	2700003
1968579454	1912369454	1849779854	1788192754	1749295754	1805733254	2242468754	2710003
2941554351	2936892751	2977388851	3003027451	3034127651	3068805951	2931435351	2720003
3149813251	3197552751	3246456951	3278347251	3232331151			2730003
9960641153							2740003
1665062554	2043891654	2036908254	2020798254	1998693254	1965062454	1926404054	2750003
1860820254	1831618654	1779266754	1722959654	1662762654	1603836054	1566825654	2760003
1620581754							2770012
1942553754	1936163054	1921424254	1899381154	1870474654	1835175454	1793595254	2780003
1748767754	1701133754	1649970654	1595361654	1541994954	1508523554	1557151454	2790003
2236528954	2219081854	2192996654	2158801054	2117052854	2067876354	2016149854	2800003
1959849054	1899285654	1834481654	1770916654	1730888454	1788998354	1788998354	2810003
2926072951	2942508951	2964492251	2992024551	3025471451	3062831351	2915237151	2820003
3150368051	3202130651	3255291151	3290031751	3239921851		2244095554	2830003
9954779353							2840003
1707639854	2079029354	2071732354	2054901754	2029726854	1996706954	1956374754	2850003
1908851554	1857599354	1803117954	1744576154	1682063654	1620944854	1582596654	2860003
1638305854							2870003
2005570354	1998702154	1982864054	1959181554	1928133954	1890233854	1845609854	2880003
1797525854	1746460954	1691647954	1633185254	1576096754	1540314254	1592305654	2890003
2216313454	2198505354	2172580854	2137738154	2095222354	2045177554	1991254654	2900012
1933971154	1872434854	1806705754	1742374554	1701949154	1760658254	1760658254	2910003
2914875251	2932095851	2955144151	2984034951	3019170651	3058465651	2903527951	2920003
3150739451	3205438051	3261718551	3298555451	3245436251		2824037454	2930003
9951784453							2940003
1721760054	2085738454	2078348854	2061307054	2035820954	2002402354	1961597654	2950003
1913539054	1861735754	1806699754	1747598754	1684532754	1622918354	1584282954	2960003
1640415354							2970003
2046576554	2019549154	2003344554	1979115554	1947354154	1908586954	1862948254	2980003
1813778654	1761570054	1705540354	1645793054	1587463854	1550910954	1604023554	2990003
2175377654	2157713154	2131309054	2096708954	2054492354	2004808554	1951290354	3000003
1894462654	1833455654	1768352654	1704714254	1664775254	1722791554	1722791554	3010003
2908829551	2926470051	2950088951	2979709251	3015752851	3056090851	2897208651	3020003
3150928251	3207221951	3265203251	3303185551	3248422951		2892212051	3030012
							3040003
							3050003
							3060003
							3070003
							3080003
							3090003
							3100003
							3110003
							3120003
							3130003
							3140003
							3150003



AXIAL & RADIAL POWER DISTRIBUTION
IN A 750 MW PBR CORE

FIG. 4.1



AXIAL & RADIAL POWER DISTRIBUTION
IN A 750 MW PBR CORE

FIG. 4.1

Figures 4.2 through 4.7 show the results of this analysis. Figure 4.2 is an axial slice along a diameter and shows lines of constant gas mass velocity through the core. The flow divergence from the high temperature regions is clearly indicated and amounts to slightly less than 10% in this case. The flow concentration in the low temperature region near the wall is also indicated. The remaining figures show the consequence of this flow divergence on the pertinent temperatures and temperature drops throughout the core.

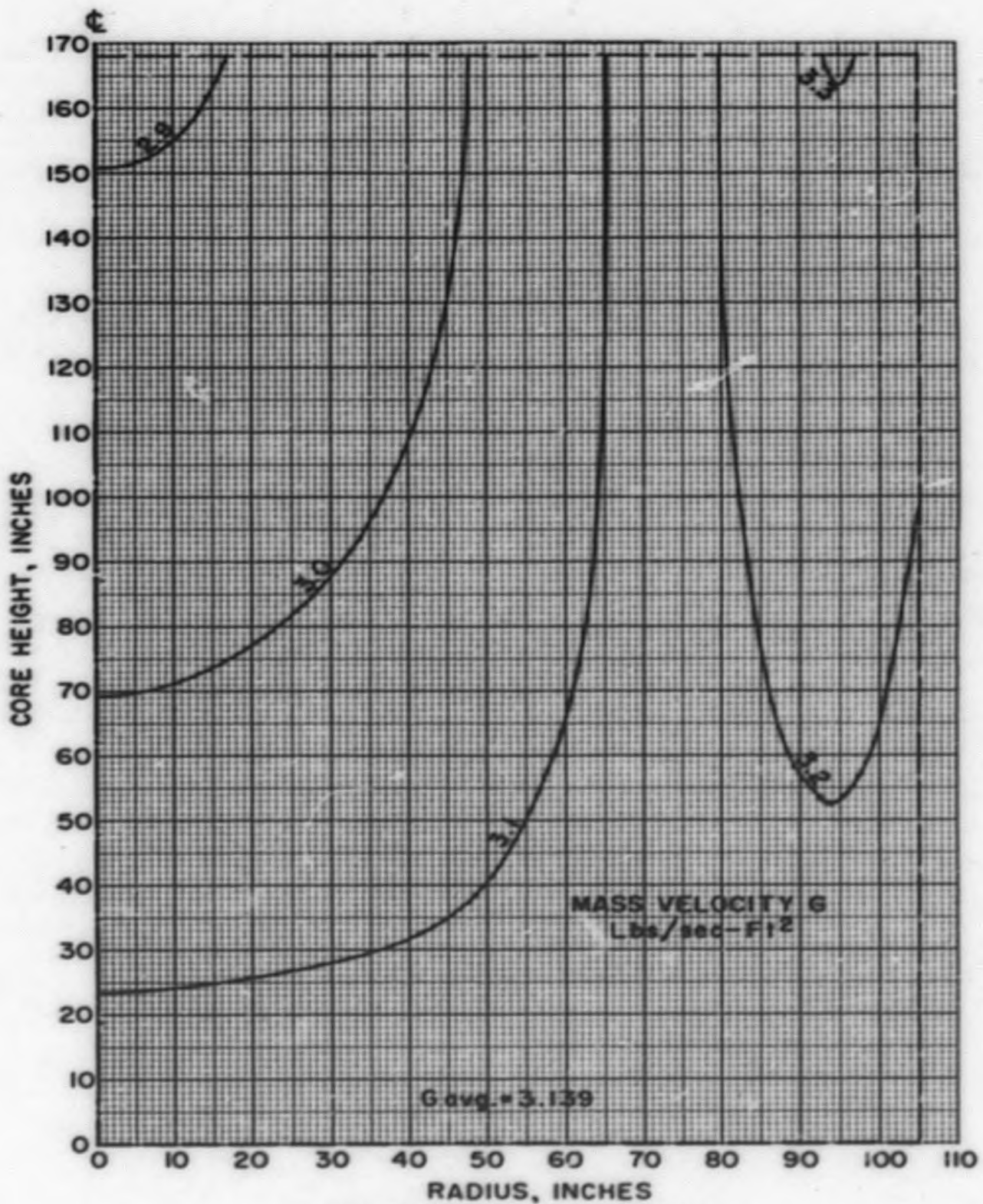
Figure 4.3 shows the change of bulk gas temperature with axial position in the core. This is obtained from the mixed mean gas output temperature leaving each axial slice.

Figure 4.4 shows the radial variation of gas temperature at the outlet end of the core and clearly indicates the high gas temperature in the region of low flow and lower gas temperature in the region of higher flow near the walls.

Figure 4.5 shows an axial slice through the core on the diameter. The region to the left of the centerline shows lines of constant graphite temperature while the region to the right of the centerline shows lines of constant gas temperature (solid) and lines of constant gas film temperature drop (broken). The relatively uniform temperature near the inlet end of the bed can be seen along with the effect of flow divergence as the gas passes through the bed.

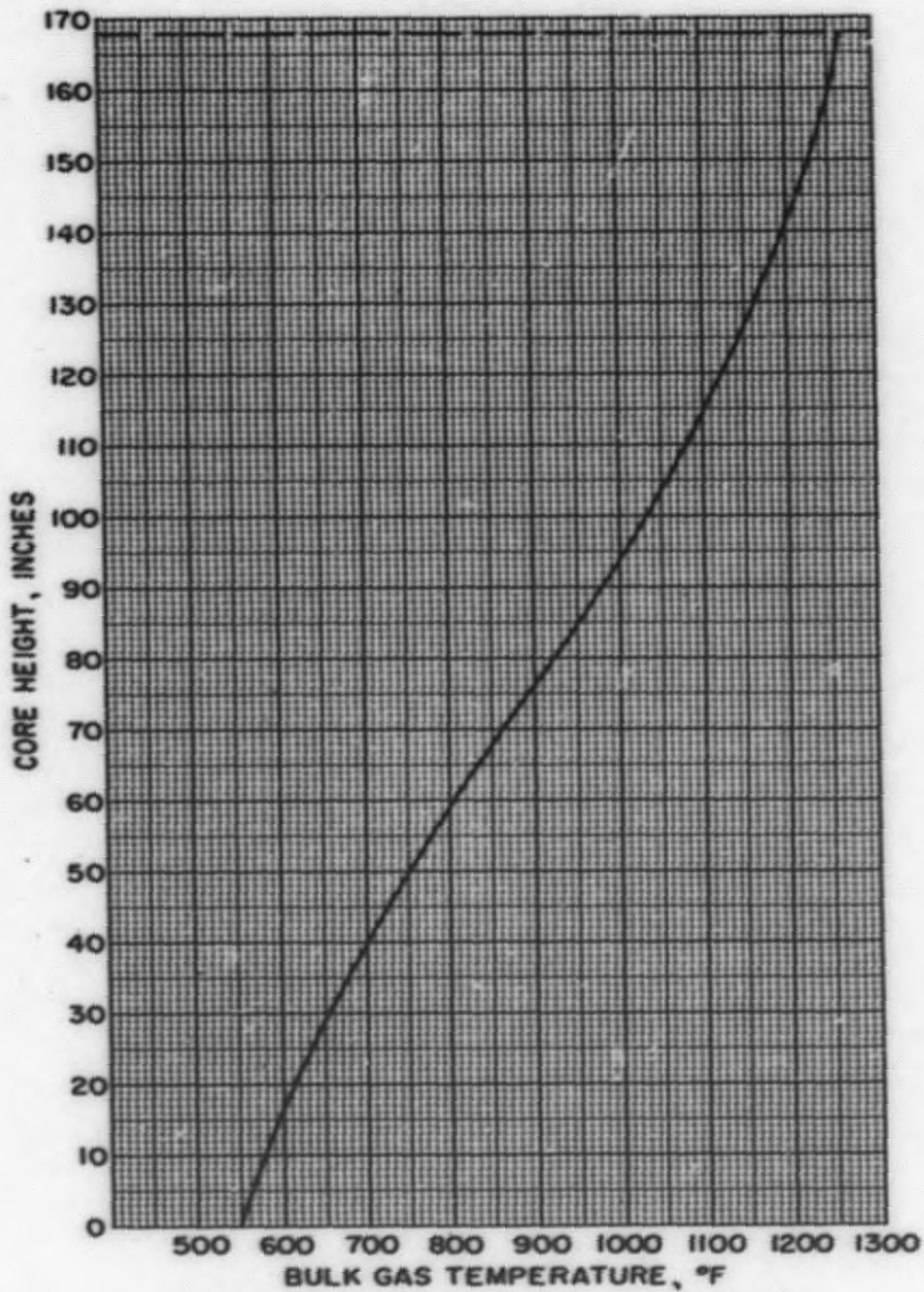
Figure 4.6 indicates the percentage of the bed which is at any indicated temperature and compares this temperature distribution with the average graphite temperature.

Figure 4.7, another axial slice through the core along the centerline, shows lines of constant ball surface temperature (solid) and lines of constant ball center temperature (dot-dash). Also shown are lines of constant ΔT_b , the temperature difference between the ball center and ball surface.



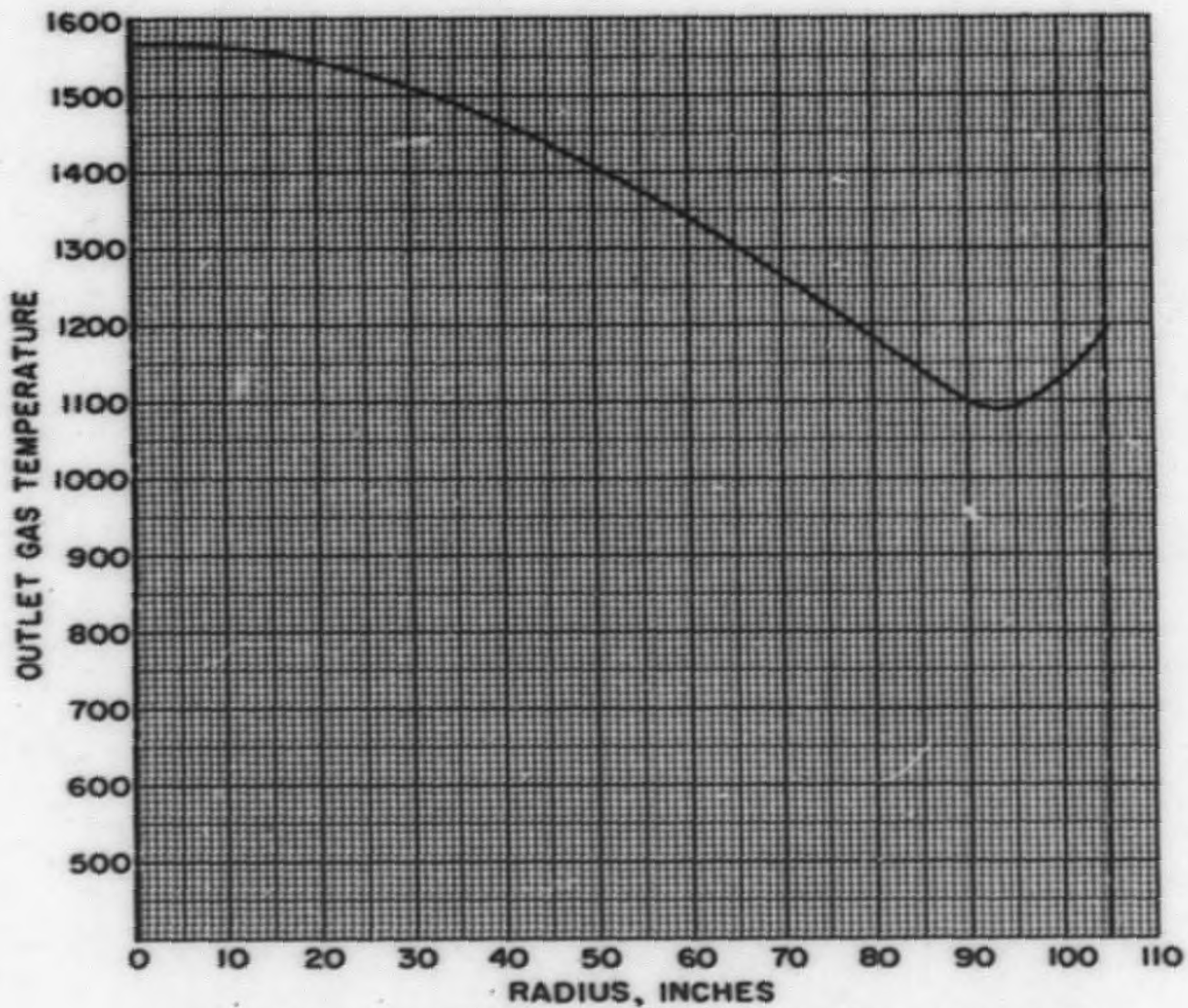
VELOCITY DISTRIBUTION
 IN A 750 MW PBR CORE

FIG. 4.2



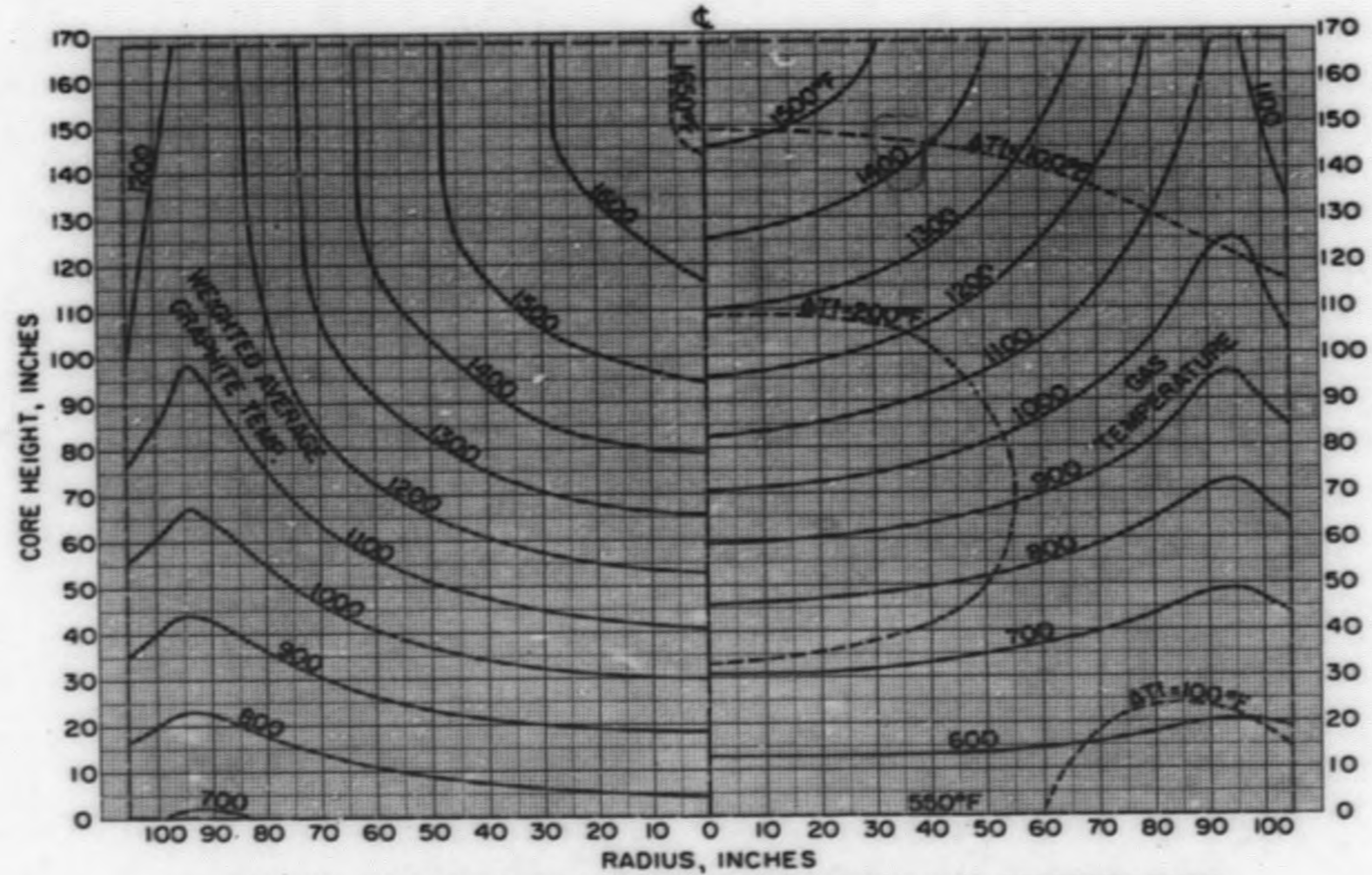
BULK GAS TEMPERATURE vs. HEIGHT
IN A 750 MW PBR CORE

FIG. 4.3



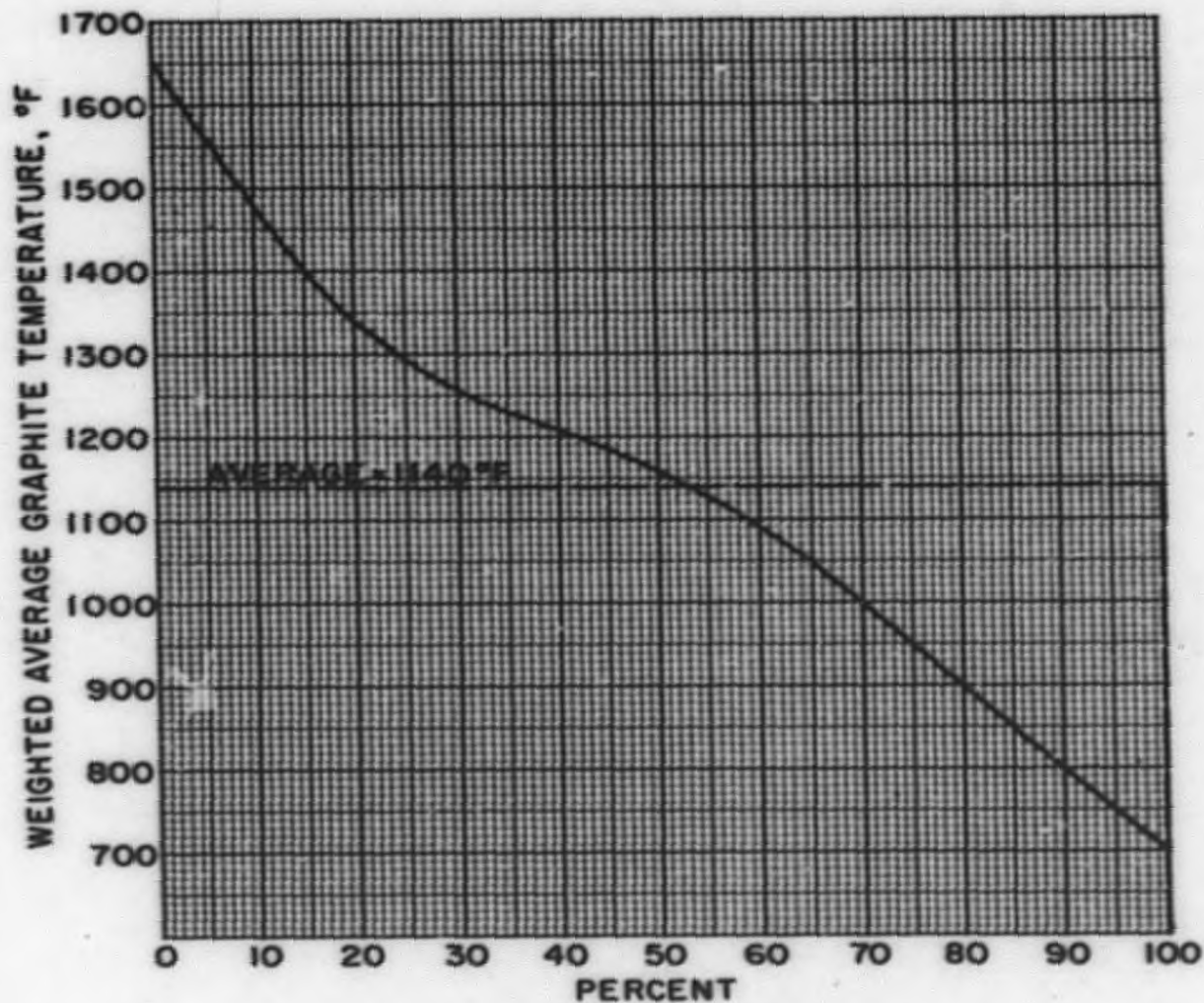
OUTLET GAS TEMPERATURE vs. RADIAL POSITION
IN A 750 MW PBR CORE

FIG. 4.4



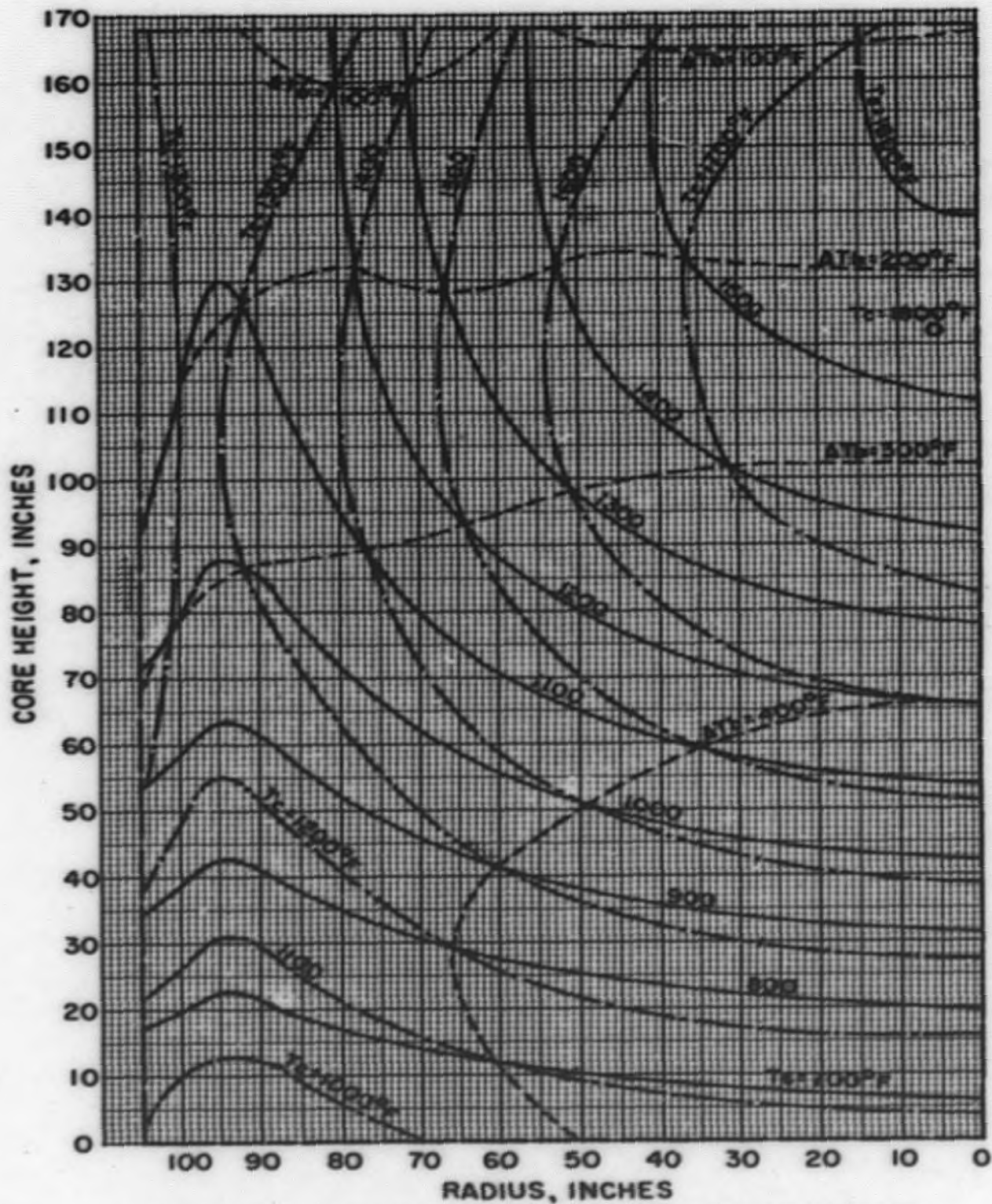
WEIGHTED AVERAGE GRAPHITE TEMPERATURE & GAS TEMPERATURE
IN A 750 MW PBR CORE

FIG. 4.5



PERCENT OF CORE
AT OR ABOVE ANY TEMPERATURE
IN A 750 MW PBR CORE

FIG. 4.6



GRAPHITE CENTER & SURFACE TEMPERATURES
IN A 750 MW PBR CORE

FIG. 4.7

COOLBALL NOMENCLATURE

<u>Symbol</u>	<u>Identification</u>
A	Frontal are, ft ²
A _i	Local frontal area region i
$\frac{\Delta P_j}{C_p}$	Normalized axial power layer j
C _p	Avg. gas heat capacity, BTU/Lb °R
C _{pX}	Heat capacity temperature exponent
D _p	Ball diameter, ft
G	Avg. mass velocity, lbs/sec/ft ²
G _{ij}	Local mass velocity, lbs/sec/ft ²
G ^{'ij}	Local mass velocity previous iteration, lbs/sec/ft ²
I	No. of axial layers
J	No. of radial regions
MW	Gas molecular weight
P	Gas pressure, psia
P _j	Outlet pressure each layer, psia
Pr	Avg. gas Prandtl number
PrX	Prandtl number temperature exponent
Q	Avg. power density, BTU/sec/ft ³ bulk volume
Q _{max}	Maximum power density, BTU/sec/ft ³ bulk volume
Q _{ij}	Local power generation, BTU/sec/ft ³ bulk volume
RP _i	Normalized radial power region i
t	Local avg. graphite temperature, °R
T _{in}	Reactor gas inlet temperature, °R
T _i	Local gas inlet temperature in any matrix cell, °R
T _{ij}	Local avg. gas temperature
ΔT_{ij}	Local gas temperature rise
\bar{T}	Core avg. gas temperature, °R
T ₂	Mixed mean outlet temperature, °R
T _{bij}	Local ball center temperature
T _{sij}	Local surface temperature, °R
W	Total gas flow rate, lbs/sec
W _i	Local gas flow rate, lbs/sec
XMU	Viscosity temperature exponent
δ	Convergence criterion on gas flow
ΔL_j	Length increment axial direction, ft.
ΔT_{fij}	Local film temperature drop
ϵ_i	Local voidage
μ	Avg. gas viscosity, lbs/ft/sec

Subscripts:

i index defining radial region
j index defining axial layer

END